mutations in each digestive tract cancer were similar: 14% (7/51) in the esophageal cancers, 15% (14/94) in the gastric cancers and 8% (11/133) in the colorectal cancers. In regard to the mutation spectrum, 30 of the 32 tumors (94%) showed deletions or insertions of 1-bp. The remaining two (6%) showed 2-bp deletions (Fig. 1).

We then compared the presence of the D310 mutations with clinicopathological features, including patient age, sex, tumor location, depth of tumor invasion, stage and lymph node metastasis in each digestive tract cancer (Tables 1–3). No significant relationships were identified in each histological type.

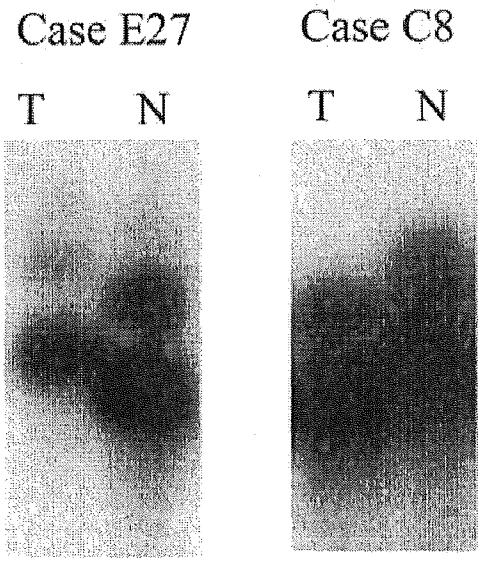

Figure 1 Representative examples of somatic mutations of the D310 repeat mtDNA by microsatellite assay. T, tumor; N, normal tissue. Case E27 shows 1-bp deletion in the tumor, and case C8 shows 1-bp insertion in the tumor.

DISCUSSION

Digestive tract cancers are the most common human malignancies and contribute to significant cancer mortality throughout the world. Digestive tract cancers comprise more than half of all malignancies in Japan.[11–13] The molecular mechanisms underlying these cancers are, however, largely unknown. The importance of mitochondria in apoptosis has been suggested in several studies.[14] Cytochrome c is released from mitochondria, an action inhibited by the presence of Bcl-2. Cytochrome c reacts with Apaf-1 and procaspase 9 and activates other caspases, leading to apoptosis. This process might be disrupted by mitochondrial dysfunction such as that which occurs with mtDNA alteration, and unlimited cell growth might occur in affected tissues. mtDNA mutations have been found in more than 40% of bladder, lung, and head and neck cancers.[7] In addition, Tan *et al.* reported that 22/27 (81%) mtDNA mutations in breast cancer occurred in the D-loop region.[15] Other reports also indicated that the D-loop region might be a hot spot for mutations.[16] This region is known to be the start site for replication of the closed, circular mitochondrial genome.[17] Replication of mtDNA begins with the synthesis of the heavy strand (H strand) with primer RNA, and the 3′ termini of primer RNA have been mapped to CSBs I-III.[18] The identification of mutations in this region indicates the necessity for further research on the mechanisms of late replication and processing of mtDNA in cancer.

Mutation frequencies of oncogenes such as K-*ras*, tumor suppressor genes *p53* and *p16* and microsatellite instability have been reported to differ between digestive tract cancers.[19–22] For example, K-*ras* mutation is frequent in colorectal cancers, but not in esophageal or

Table 1 Relationship between mtDNA mutations and clinicopathological characteristics of esophageal cancer

	Mutation in D310			
Characteristics	Positive	Negative	NI	Frequency of mutation
Patient age				
<65 years	5	18	2	22%
≥65 years	2	26	6	7%
Sex				
Male	5	37	8	12%
Female	2	7	0	22%
Tumor location				
Upper	0	4	0	0%
Middle	5	28	6	15%
Lower	2	12	2	14%
Depth of invasion				
Mucosa/submucosa	3	16	4	16%
Muscularis propria	4	28	4	13%

NI, not informative.

Table 2 Relationship between mtDNA mutations and clinicopathological characteristics of gastric cancer

Characteristics	Mutation in D310			Frequency of mutation
	Positive	Negative	NI	
Patient age				
<65 years	6	34	0	15%
≥65 years	8	46	2	15%
Sex				
Male	11	56	1	16%
Female	3	24	1	11%
Tumor location				
Upper	4	26	0	13%
Lower	10	54	2	16%
Histological type				
Intestinal	11	57	2	16%
Diffuse	3	23	0	12%
Depth of invasion				
Mucosa/submucosa	8	52	0	13%
Muscularis propria	6	28	2	18%
Lymph node metastasis				
Negative	12	57	1	17%
Positive	2	23	1	8%

NI, not informative.

Table 3 Relationship between mtDNA mutations and clinicopathological characteristics of colorectal cancer

Characteristics	Mutation in D310			Frequency of mutation
	Positive	Negative	NI	
Patient age				
<65 years	4	63	2	6%
≥65 years	7	59	3	11%
Sex				
Male	7	75	3	9%
Female	4	47	2	8%
Tumor location				
Right	3	29	1	9%
Left	8	93	4	8%
Depth of invasion				
<ss	3	37	3	8%
≥ss	8	85	2	9%
Lymph node metastasis				
Negative	4	64	1	6%
Positive	7	58	4	11%

NI, not informative; ss, subserosa.

gastric cancers. Microsatellite instability is frequent in colorectal and gastric cancers but not in esophageal cancers. Methylation patterns also differ among the cancers.[23] These results suggest that these cancers might develop through different pathways. However, most cancers show telomerase activity, which is important for cell immortality. To clarify the role of mtDNA mutations in digestive tract cancers, analyses of the frequency and spectrum of the mutations are crucial. However, few researchers have examined mtDNA alterations in the digestive tract cancers. In addition, the reported frequencies of the mutation of mtDNA in digestive tract cancers were various, from 5% to 34% in the esophageal cancers,[5,24,25] from 4% to 18% in the gastric cancers,[26–28] and from 44% to 66% in the colorectal cancers.[3,27,29] This could possibly be a result of the differences of method and locus examined. We therefore examined only the D310 locus by one method, microsatellite analysis, in each digestive tract cancer. Frequencies of mtDNA mutations were similar

in each digestive tract cancer in the present study. We also found that there were no significant relationships between mtDNA mutations and clinicopathological features, including patient age, sex, tumor location, depth of tumor invasion, stage and lymph node metastasis in each digestive tract cancer. In several other cancers, no correlations between mtDNA mutations and clinicopathological features have been identified.[30] This suggests that mtDNA mutations play a role in the development but not progression in each digestive tract cancer, and that the role of mtDNA mutations might be similar among the digestive tract cancers.

A large number of mtDNA mutations have been reported in not only cancer cells, but also human somatic tissues during aging. These mutations include large deletions, point mutations and small deletions. It is important to note that mtDNA mutations reported during aging are mosaic, that is, there is uneven distribution of particular mutant mtDNA molecules among the cells of a given tissue. This is because of the intrinsic heteroplasmic nature of the mtDNA population in cells. It is likely that increased susceptibility of mtDNA to oxidative damage and limited DNA repair capacity of the proteins involved in mitochondrial repair play a significant role in mutagenesis in aging. The mitochondrial dysfunction that accompanies aging might exert a major influence on carcinogenesis. Further examinations are necessary to clarify the issue.

ACKNOWLEDGMENTS

We thank Ms K Kunimitsu and N Kubota for technical assistance.

REFERENCES

1 Larsson NG, Clayton DA. Molecular genetic aspects of human mitochondrial disorders. *Annu. Rev. Genet.* 1995; **29**: 151–78.
2 Chinnery PF, Turnbull DM. Mitochondrial DNA and disease. *Lancet* 1999; **354**: 17–21.
3 Habano W, Nakamura S, Sugai T. Microsatellite instability in the mitochondrial DNA of colorectal carcinomas: evidence for mismatch repair systems in mitochondrial genome. *Oncogene* 1998; **17**: 1931–7.
4 Sanchez-Cespedes M, Parrella P, Nomoto S *et al.* Identification of a mononucleotide repeat as a major target for mitochondrial DNA alterations in human tumors. *Cancer Res.* 2001; **61**: 7015–19.
5 Hibi K, Nakayama H, Yamazaki T *et al.* Mitochondrial DNA alteration in esophageal cancer. *Int. J. Cancer* 2001; **92**: 319–21.
6 Parrella P, Xiao Y, Fliss M *et al.* Detection of mitochondrial DNA mutations in primary breast cancer and fine-needle aspirates. *Cancer Res.* 2001; **61**: 7623–6.
7 Fliss MS, Usadel H, Caballero OL *et al.* Facile detection of mitochondrial DNA mutations in tumors and bodily fluids. *Science* 2000; **287**: 2017–19.
8 Lauren P. The two histological main types of gastric carcinoma: diffuse and so-called intestinal type carcinoma. An attempt at a histoclinical classification. *Acta Pathol. Microbiol. Scand.* 1965; **64**: 31–49.
9 *Japanese Gastric Cancer Association classification of gastric carcinoma.* Tokyo: Kanehara, 1995.
10 Miyoshi E, Haruma K, Hiyama T *et al.* Microsatellite instability is a genetic marker for the development of multiple gastric cancers. *Int. J. Cancer* 2001; **95**: 350–53.
11 Marugame T, Hamashima C. Mortality trend of esophageal cancer in Japan: 1960–2000. *Jpn J. Clin. Oncol.* 2003; **33**: 491–2.
12 Kaneko S, Yoshimi I. Mortality trend of stomach cancer in Japan: 1960–2000. *Jpn J. Clin. Oncol.* 2003; **33**: 105–6.
13 Marugame T, Hamashima C. Mortality trend of colon cancer in Japan: 1960–2000. *Jpn J. Clin. Oncol.* 2003; **33**: 320–21.
14 Green DR, Reed JC. Mitochondria and apoptosis. *Science* 1998; **281**: 1309–12.
15 Tan DJ, Bai RK, Wong LJC. Comprehensive scanning of somatic mitochondrial DNA mutations in breast cancer. *Cancer Res.* 2002; **62**: 972–6.
16 Michikawa Y, Mazzucchelli F, Bresolin N *et al.* Aging-dependent large accumulation of point mutations in the human mtDNA control region for replication. *Science* 1999; **286**: 774–9.
17 Clayton D. Replication and transcription of vertebrate mitochondrial DNA. *Annu. Rev. Cell Biol.* 1991; **7**: 453–78.
18 Chang DD, Clayton DA. Priming of human mitochondrial DNA replication occurs at the light-strand promoter. *Proc. Natl. Acad. Sci. USA* 1985; **82**: 351–5.
19 Lutz WK, Fekete T. Vamvakass. Position- and base pair-specific comparison of p53 mutation spectra in human tumors: elucidation of relationships between organs for cancer etiology. *Environ. Health Perspect.* 1998; **106**: 207–11.
20 Igaki H, Sasaki H, Tachimori Y *et al.* Mutation frequency of the p16/CDKN2 gene in primary cancers in the upper digestive tract. *Cancer Res.* 1995; **55**: 3421–3.
21 Victor T, Du Toit R, Jordaan AM *et al.* No evidence for point mutations in codon 12, 13, and 61 of the ras gene in a high-incidence area for esophageal and gastric cancer. *Cancer Res.* 1990; **50**: 4911–14.
22 Dai CY, Furth EE, Mick R *et al.* p16 (INK4a) expression begins early in human colon neoplasia and correlates inversely with markers of cell proliferation. *Gastroenterology* 2000; **119**: 929–42.
23 Hibi K, Nakayama H, Kanyama Y *et al.* Methylation pattern of HLTF gene in digestive tract cancers. *Int. J. Cancer* 2003; **104**: 433–6.
24 Kumimoto H, Yamane Y, Nishimoto Y *et al.* Frequent somatic mutations of mitochondrial DNA in esophageal squamous cell carcinoma. *Int. J. Cancer* 2004; **108**: 228–31.
25 Miyazono F. Mutations in the mitochondrial DNA D-loop region occur frequently in adenocarcinoma in Barrett's esophagus. *Oncogene* 2002; **21**: 3780–83.
26 Habano W, Sugai T, Nakamura S *et al.* Microsatellite instability and mutation of mitochondrial and nuclear DNA in gastric carcinoma. *Gastroenterology* 2000; **118**: 835–41.
27 Bianchi NO, Bianchi MS, Richard SM. Mitochondrial genome instability in human cancers. *Mut. Res.* 2001; **488**: 9–23.

28 Tamura G, Nishizuka S, Maesawa G *et al.* Mutations in mitochondrial control region DNA in gastric tumors of Japanese patients. *Eur. J. Cancer* 1999; **35**: 316–19.

29 Polyak K, Li Y, Zhu H *et al.* Somatic mutations of the mitochondrial genome in human colorectal tumours. *Nat. Genet.* 1998; **20**: 291–3.

30 Coller HA, Khrapko K, Bodyak ND *et al.* High frequency of homoplasmic mitochondrial DNA mutations in human tumors can be explained without selection. *Nat. Genet.* 2001; **28**: 147–50.

Suberoylanilide Hydroxamic Acid Enhances Gap Junctional Intercellular Communication via Acetylation of Histone Containing *Connexin 43* Gene Locus

Takahiko Ogawa,[1] Tomonori Hayashi,[1] Masahide Tokunou,[1] Kei Nakachi,[1] James E. Trosko,[3] Chia-Cheng Chang,[3] and Noriaki Yorioka[2]

[1]Department of Radiobiology and Molecular Epidemiology, Radiation Effects Research Foundation; [2]Department of Molecular and Internal Medicine, Graduate School of Biomedical Sciences, Hiroshima University, Hiroshima, Japan; and [3]National Food Safety Toxicology Center, Department of Pediatrics/Human Development, Michigan State University, East Lansing, Michigan

Abstract

A histone deacetylase (HDAC) inhibitor, suberoylanilide hydroxamic acid (SAHA), induces apoptosis in neoplastic cells, but its effect on gap junctional intercellular communication in relation to apoptosis was unclear. Therefore, we carried out a comparative study of the effects of two HDAC inhibitors, SAHA and trichostatin-A, on gap junctional intercellular communication in nonmalignant human peritoneal mesothelial cells (HPMC) and tumorigenic *ras* oncogene–transformed rat liver epithelial cells (WB-ras) that showed a significantly lower level of gap junctional intercellular communication than did HPMC. Gap junctional intercellular communication was assessed by recovery rate of fluorescence recovery after photobleaching. Treatment of HPMC with SAHA at nanomolar concentrations caused a dose-dependent increase of recovery rate without inducing apoptosis. This effect was accompanied by enhanced connexin 43 (*Cx43*) mRNA and protein expression and increased presence of Cx43 protein on cell membrane. Trichostatin-A induced apoptosis in HPMC but was less potent than SAHA in enhancing the recovery rate. In contrast, treatment of WB-ras cells with SAHA or trichostatin-A induced apoptosis at low concentrations, in spite of smaller increases in recovery rate, *Cx43* mRNA, and protein than in HPMC. Chromatin immunoprecipitation analysis revealed that SAHA enhanced acetylated histones H3 and H4 in the chromatin fragments associated with *Cx43* gene in HPMC. These results indicate that SAHA at low concentrations selectively up-regulates *Cx43* expression in normal human cells without induction of apoptosis, as a result of histone acetylation in selective chromatin fragments, in contrast to the apoptotic effect observed in tumorigenic WB-ras cells. These results support a cancer therapeutic and preventive role for specific HDAC inhibitors. (Cancer Res 2005; 65(21): 9771-8)

Introduction

Histone deacetylase (HDAC) inhibitors have been suggested as potential cancer therapeutic agents because of their different effect on apoptosis in normal and cancer cells (1, 2). The prototype of hydroxamic acid–based hybrid polar molecules, suberoylanilide hydroxamic acid (SAHA), belongs to the second generation of this class of potential therapeutic cancer drugs. It displays a greater potency, on a molar basis, as an inducer of differentiation and, therefore, is expected to be a safer analogue of trichostatin-A (3, 4). SAHA functions as a HDAC inhibitor, with ID_{50} values close to its optimal differentiation-inducing concentration (5). Acetylation of core nucleosomal histones is, in part, regulated by opposing activities of histone acetyltransferases and HDACs (6, 7); the increased acetylation of histones is associated with genes that are transcriptionally activated (8, 9). Hyperacetylation induced by HDAC inhibitors, such as SAHA, seems to be highly selective and changed the expression of only 2% to 5% of all genes (10). SAHA induces differentiation and/or apoptosis in certain transformed cells through the increased expression of selected genes involved in the cell cycle regulation, tumor suppression, differentiation, and apoptosis (5, 6). It has been reported that increased gene expression of the cell cycle kinase inhibitor $p21^{WAF1}$ might account for the antitumor property of SAHA (6, 11), but the precise mechanism remains to be elucidated.

Asklund et al. (12) recently reported that 4-phenylbutyrate, an HDAC inhibitor, enhances gap junctional intercellular communication through increased levels of connexin 43 (Cx43) in malignant glioma cells, although precisely how this HDAC inhibitor up-regulates Cx43 has not been delineated. We previously reported that hexamethylene bisacetamide (HMBA), a hybrid polar molecule, enhanced gap junctional intercellular communication in human peritoneal mesothelial cells (HPMC), which are nontumorigenic primary cultured cells. This effect, induced by millimolar concentrations, was accompanied by an increased expression of both mRNA and phosphorylated isoforms of Cx43 (13, 14). Side effects, such as myelotoxicity, have been reported for HMBA (15).

Gap junction channels transport small molecules (<2,000 Da) important in growth regulation signaling between neighboring cells (16, 17). Gap junctional intercellular communication is involved in cell growth, differentiation, and apoptosis; aberrant control of gap junctional intercellular communication might also play an important role in cancer development (18–21). Several oncogene products have been shown to reduce gap junction channel permeability and connexin expression *in vitro* and *in vivo* (22, 23). It is anticipated that SAHA will work as an enhancer of gap junctional intercellular communication in both normal and cancer cells. It is then important to elucidate (*a*) whether SAHA enhances Cx43 expression and gap junctional intercellular communication in normal human cells and neoplastically transformed cells, with specific target molecules at lower concentrations than with trichostatin-A; (*b*) whether apoptosis is induced also in

Note: T. Ogawa and T. Hayashi contributed equally to this work.

Requests for reprints: Takahiko Ogawa or Tomonori Hayashi, Department of Radiobiology and Molecular Epidemiology, Radiation Effects Research Foundation, 5-2, Hijiyama Park, Minami Ward, 732-0815 Hiroshima, Japan. Phone: 81-82-261-3131; Fax: 81-82-261-3170; E-mail: tk-ogawa@hph.pref.hiroshima.jp or tomo@rerf.or.jp.

doi:10.1158/0008-5472.CAN-05-0227

normal cells or only in neoplastic cells; and (*c*) if so, what the specific mechanisms are. Therefore, this study assesses the effects of SAHA, an HDAC inhibitor, on Cx43 expression and apoptosis in normal and neoplastically transformed cells, from the view of cancer prevention and cancer chemotherapy, along with the underlying molecular mechanisms.

Materials and Methods

Cells. HPMC was harvested from the omental tissues of three consenting patients who had undergone elective abdominal surgery. As described previously, the cells were isolated and cultured in M199 medium, supplemented with L-glutamine, 10% FCS (Intergen, Co., Purchase, NY), penicillin, and streptomycin. All experiments were done using the initial primary culture or the third-passage cells. A cell line previously derived from WB-F344 rat liver epithelial cells was also used in this study (24). WB-ras cells are a neoplastically transformed line originating from infection of WB-F344 rat liver epithelial cells with retrovirus (raszip6) containing viral Ha-*ras* and the neomycin-resistant gene (25). WB-ras cells were cultured in MEM medium, supplemented with L-glutamine, sodium pyruvate, essential amino acid, nonessential amino acid, MEM-vitamin solution, 7% FCS (Intergen), penicillin, and streptomycin.

Drugs and chemicals. SAHA was kindly provided by Aton Pharma, Inc. (Tarrytown, NY). Trichostatin-A, DMSO, and bovine serum albumin (BSA) were purchased from Sigma Chemical Co. (St. Louis, MO). Trichostatin-A and SAHA were prepared in a 100 mmol/L stock solution in DMSO and stored at −20°C.

Experimental design. Cells were seeded at a density of $1.0 \times 10^4/cm^2$ in growth medium. After confluence was reached, SAHA or trichostatin-A was added and the culture was continued, whereas DMSO was used as solvent control. The incubation times and the concentrations of SAHA or trichostatin-A used were based on the results of earlier studies (5–7, 26–28). Cells in the present study were incubated for 48 hours at 37°C with 50, 200, 800, and 2,000 nmol/L SAHA or trichostatin-A. These cells were then used for cell proliferation and apoptosis assays. Measurements of gap junctional intercellular communication and assessment of Cx43 protein and acetylated histones H3 and H4 were done by Western blotting and immunocytochemistry, along with mRNA quantitative analyses and chromatin immunoprecipitation assays. The $p21^{WAF1}$ protein levels were also assessed.

Analysis of cell growth and cell cycle. To assess the effect of SAHA on cell proliferation, viable cells were stained with a tetrazolium salt, 4-[3-(4-iodophenyl)-2-(4-nitrophenyl)-2*H*-5-tetrazolio]-1,3-benzene disulfonate (WST-1, Dojindo Laboratories, Kumamoto, Japan; ref. 29). In the present experiments, HPMC was seeded at a density of 5.0×10^3 per well in a 96-well plate. After culture for 24 hours, the cells were exposed to the medium containing SAHA or DMSO. SAHA was added to basal medium at final concentrations of 50, 200, 800, and 2,000 nmol/L; staining was done after 24 and 48 hours. The absorbance at 450 nmol/L (with reference at 650 nmol/L) was measured with microtiter plate spectrophotometer (EXPERT 98, ASYS HITEC GmbH, Linz, Austria). The results are expressed as the ratios of viable treated cells compared with the untreated control sample (arbitrary 1 unit). For cell cycle analysis, cells were trypsinized, slowly resuspended in 70% ethanol in PBS at 4°C for 5 minutes, washed in PBS, and incubated for 30 minutes in PBS containing 0.05 mg/mL propidium iodide (Sigma), and 1 mg/mL RNaseI (Sigma). The cell suspension was then analyzed on flow cytometry (BD Biosciences, San Jose, CA).

Assessment of apoptosis by Annexin V/propidium iodide staining. Cells were stained with FITC-labeled Annexin V for exposure of phosphatidylserine on the cell surface as an indicator of apoptosis using a FACScan flow cytometer, following the instructions of the manufacturer (BD Biosciences). Briefly, SAHA- or trichostatin-A–treated cells (5×10^5-10×10^5) for 24 and 48 hours were collected by centrifugation at $3,500 \times g$ for 2 minutes and washed with 500 μL of PBS with 1% FCS thrice. The washed cells were resuspended in 180 μL PBS with 1% FCS and 0.5 μL FITC-labeled Annexin V and 1 μL propidium iodide, from MEBCYTO Apoptosis kit (MBL, Nagoya, Japan), were added to the cell suspension. After reaction for 5 minutes at room temperature, 10,000 cells were analyzed with FACScan. Obtained data were processed to the quadrant population analysis, using CellQuest software (BD Biosciences). The living cell population was determined as cells that were negative for both Annexin V and propidium iodide (distributed in the lower left of quadrant). The results are expressed as the percentage of living cell numbers.

Fluorescence recovery after photobleaching assay for gap junctional intercellular communication. The procedure was a modified version of the standard method for measuring gap junctional intercellular communication by quantitative fluorescence recovery after photobleaching (30, 31). Assays were done using an ACAS Ultima laser cytometer (Meridian Instruments, Inc., Okemos, MI). After bleaching of randomly selected cells with a microlaser beam, the rate of transfer of 5,6-carboxyfluorescein diacetate (Molecular Probes, Inc., Eugene, OR) from the adjacent labeled cells back into bleached cells was calculated. Recovery of fluorescence was examined after 0.5 minute and the recovery rate was calculated as percentage per minute (i.e., the percentage of photobleached fluorescence). The recovery rate was corrected for the loss of fluorescence measured in unbleached cells, and results are expressed as the ratio (mean ± SD) of recovery rate relative to that of untreated control cells.

Extraction of *Cx43* RNA. Cells were grown in 6 cm dishes and were prepared as described previously. In brief, after 48 hours of incubation, the cells were trypsinized and suspended in M199 medium containing 10% FCS or MEM containing 7% FCS. After cells were washed once with PBS, 100 μL RNAlater (Ambion, Austin, TX) was added to pellets, which were then stored in a freezer until use. Total RNA was isolated from cells by using QIAshredder and RNeasy Mini kits (Qiagen, Inc., Chatsworth, CA). The initial strand of cDNA was synthesized from 500 ng of RNA extracts in a volume of 20 μL using avian myeloblastosis virus reverse transcriptase XL (TaKaRa, Otsu, Japan) priming with random 9-mers at 42°C for 10 minutes. The cDNA strand was stored at −20°C until use. Expression of *hCx43* and *rCx43* mRNAs was evaluated by real-time reverse transcription-PCR (RT-PCR) based on the TaqMan method. In brief, PCR was done in an ABI PRISM 7900 sequence detector (Perkin-Elmer/Applied Biosystems, Foster City, CA) in a final volume of 20 μL. The PCR mixture contained 10 mmol/L Tris-HCl buffer (pH 8.3; Perkin-Elmer/Applied Biosystems), 50 mmol/L KCl, 1.5 mmol/L $MgCl_2$, 0.2 mmol/L deoxynucleotide triphosphate mixture, 0.5 units of AmpliTaq Gold (Perkin-Elmer/Applied Biosystems), 0.2 μmol/L primers, and probe. The primer and probe sequences for gene amplification were as follows: (*a*) *hCx43*, 5-GGAAAGAGCGACCCTTACCAT-3 (forward primer), 5-AGGAGCAGCCATTGAAATAAGCATA-3 (reverse primer), and 5-CTGAGCCCTGCCAAAGA-3 (probe); (*b*) glyceraldehyde-3-phosphate dehydrogenase (*GAPDH*): the housekeeping gene, 5-AATTCCATGG-CACCGTCAA-3 (forward primer), 5-CCAGCATCGCCCCACTT-3 (reverse primer), and 5-CC ATCACCATCTTCCAGGAGCGA GA-3 (probe); (*c*) *rCx43*; 5-ATCAGCATCCTCTTCAAGTCTGTCT-3 (forward primer), 5-CAGG-GATCTCTCTTGCAGGTGTA-3 (reverse primer), and 5-CCTGCTCATC-CAGTGGT-3 (probe). The TaqMan probes carried a 5-FAM reporter label, and 3′ minor groove binder and nonfluorescence quencher groups were synthesized by Applied Biosystems. The determination of *rGAPDH* used the TaqMan rodent GAPDH control reagents (Applied Biosystems). The AmpliTaq Gold enzyme was activated by heating for 10 minutes at 95°C and all genes were amplified by a first step of heating for 15 seconds at 95°C followed by 1 minute at 60°C for 50 cycles.

Quantification for *Cx43* messenger RNA. For the construction of standard curves of positive controls, the total RNA of HPMC was reverse-transcribed into cDNA and serially diluted in water in 5 or 6 log steps to give 4-fold serial dilutions of cDNA from ~100 ng to 100 pg. This cDNA serial dilution was prepared once for all examinations done in this study and stored at −20°C. The coefficient of linear regression (r) for each standard curve was calculated. When the cycle threshold value of a sample was substituted in the formula for each standard curve, the relative concentration of *hCx43*, *GAPDH*, *rCx43*, or *rGAPDH* could be calculated. To normalize for differences in the amount of total RNA added to each reaction mixture, *GAPDH* was selected as an endogenous RNA control. The data

represent the average expression of target genes: expression relative to *GAPDH* ± SD from three independent cultures.

Immunoblotting. Cells were grown to confluence in 6 cm dishes and were cultured with SAHA or DMSO. At the end of the given treatment period, the monolayers were rinsed thrice with ice-cold PBS and disposed of according to the extraction method. Nuclear extracts: Trypsinized cells were washed in PBS and resuspended in cell lysis buffer of Nuclear/Cytosol Fractionation Kit (BioVision, Inc., Mountain View, CA) and cells were then treated according to the protocol of the manufacturer. Whole cell samples: Lysates were prepared with ice-cold lysis buffer containing 20 mmol/L TBS (pH 7.5); 1% Triton X-100; 150 mmol/L NaCl; and 1 mmol/L each of EDTA, EGTA, β-glycerophosphate, Na_3VO_4, and phenylmethylsulfonyl fluoride, 2.5 mmol/L sodium PPi, and 1 μg/mL leupeptin. The lysates were then sonicated. The samples were diluted 1:4 in water, and their protein concentrations were determined using detergent-compatible protein assay (Bio-Rad Corp., Richmond, CA). Samples (30 μg for Cx43, 15 μg for histones and $p21^{WAF1}$) of protein were then dissolved in Laemmli sample buffer, separated on 12.5 (for Cx43) and 15% polyacrylamide gels (for acetylated histones H3/H4 and $p21^{WAF1}$), and transferred to polyvinylidene difluoride (PVDF) membranes (Bio-Rad). As an internal control to determine whether equal amounts of protein had been loaded on to the gel, the PVDF membranes were stripped and reprobed with anti-α-tubulin (T5168, Sigma) mouse monoclonal antibody ($p21^{WAF1}$ and Cx43). After being washed with distilled water, the membranes were scanned with a flathead scanner, and total band density as amount of loaded protein was analyzed by NIH Image. The Cx43, acetylated histones H3/H4, or $p21^{WAF1}$ contents of the various samples were determined by incubating them with anti-Cx43 monoclonal antibody (diluted 1:2,000; Chemicon International, Inc., Temecula, CA), antiacetylated histone H3 or H4 antibody (diluted 1:1,000; Upstate Biotechnology, Lake Placid, NY), and anti-$p21^{WAF1}$ protein monoclonal antibody (F-5; Santa Cruz Biotechnology, Inc., Santa Cruz, CA). Next, a horseradish peroxidase–conjugated secondary antibody (diluted 1:2,000; Amersham Co., Arlington Heights, IL) and an enhanced chemiluminescence detection reagent (Renaissance Western blot chemiluminescence reagent; NEN Life Science Products, Inc., Boston, MA) were added. The average control value was assigned an arbitrary value of 1 unit, and relative band intensities were standardized to this arbitrary unit. Exposed films were scanned using a flathead scanner, and band density was quantified by NIH Image.

Indirect immunofluorescence and confocal microscopy. HPMC and WB-ras cells were cultured as described previously. The cells were plated on a Lab-Tek Chamber Slide (Nalge Nunc Int., Naperville, IL) before culture with SAHA or DMSO. The cells were then washed twice in PBS and fixed in 95% methanol/5% acetic acid for 1 minute at room temperature before being washed and permeabilized thrice with 0.1% Triton X-100–PBS (PBST), and then incubated in 5% BSA for 60 minutes. After this, slides were incubated overnight at 4°C in anti-Cx43 monoclonal antibody (Chemicon) at a 1:400 dilution, and antiacetylated histone H3 polyclonal antibody at a 1:200 dilution (Upstate Biotechnology). Next, the cells were washed thrice with PBST and incubated in Alexa 546–conjugated goat anti-mouse antibody and Alexa 488–conjugated goat anti-rabbit antibody (Molecular Probes) at a dilution of 1:500 for 1 hour, in dark conditions. The slides were then washed thrice in PBST and once in PBS before being mounted in Gel/Mount (Biomeda, Corp., Foster City, CA). Finally, the cells were examined by Zeiss LSM 510 laser-scanning confocal microscope (Carl Zeiss International, Jena, Germany).

Chromatin immunoprecipitation assay. HPMC was plated at a density of 2×10^6 cells/6 cm dish and incubated overnight at 37°C with 5% CO_2. The next day, cells were cultured with SAHA (2,000 nmol/L) for 0, 2, or 24 hours. Chromatin immunoprecipitation assay was done according to the protocol of the manufacturer (32). DNA extracted from both

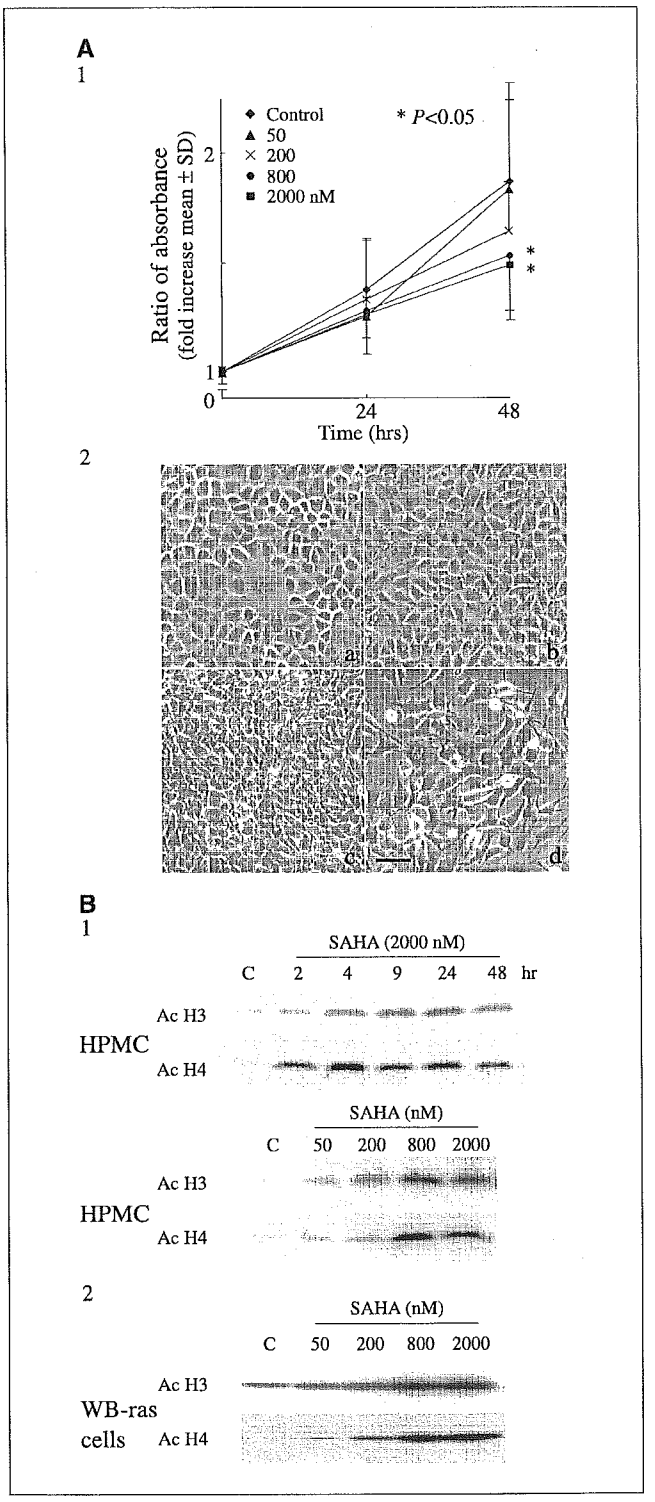

Figure 1. SAHA-induced growth suppression occurred only at high concentrations, and SAHA induced neither morphologic changes nor apoptosis even with accumulation of acetylated histones in HPMC. *A1*, SAHA time course and dose response in HPMC. Viable cell number was analyzed by WST-1 assay. Measurement at each time point was done in quadruplet. *Points*, mean; *bars*, SD. *A2*, phase-contrast micrographs. HPMC and WB-ras cells were cultured on Lab-Tek chamber slides with (*b* and *d*) or without (*a* and *c*) SAHA (2,000 nmol/L) for 48 hours. *Bar*, 100 μm. *B*, Western blot analysis of acetylated histones H3 and H4 in HPMC. Histones were isolated by nuclear extraction as described in Materials and Methods from the cells cultured for indicated hours and with indicated concentrations of SAHA (*B1*). Acetylation was detected by using antiacetylated H3 and H4 antibodies. *Lane C*, untreated HPMC or WB ras cells (control).

immunoprecipitation steps was purified by phenol/chloroform extraction and ethanol precipitation, and analyzed by real-time RT-PCR. The same *Cx43* primers and probe for the real-time RT-PCR analysis were used to carry out real-time PCR of *Cx43* DNA with samples obtained from chromatin immunoprecipitation experiments. The amplification and detection procedures were identical to the real-time RT-PCR analysis.

Statistical analysis. Data were analyzed using Statview II software (Apple Computer, Inc., Cupertino, CA). The two-tailed unpaired *t* test was used in comparing SAHA-treated cultures with control cultures; differences were considered significant at $P < 0.05$. Results are expressed as the mean ± SD.

Results

Suberoylanilide hydroxamic acid inhibits human peritoneal mesothelial cell growth without inducing morphologic changes. Figure 1*A1* shows the results of the WST-1 assay of viable cell numbers. In preliminary experiments, WST-1 staining of HPMC (i.e., absorbance at 450 nm) was found to increase linearly with the number of viable cells from 1×10^3 to 1×10^5 per well in a 96-well plate (data not shown). SAHA, at 800 and 2,000 nmol/L, seemed to suppress cell proliferation of HPMC when compared with the cells incubated in the untreated control, but this was not associated with any loss of cell viability as determined by trypan blue exclusion (data not shown). Phase-contrast micrographs of control confluent HPMC revealed uniform monolayers of polygonal cells that clearly exhibited contact inhibition (Fig. 1*A2, a*); SAHA (2,000 nmol/L) did not change morphology of the HPMC even after 48 hours (Fig. 1*A2, b*). On the other hand, WB-ras cells revealed spindle-shaped morphologies and loss of contact inhibition (Fig. 1*A2, c*), and some of these cells became rounded with detached from the dishes (Fig. 1*A2, d*).

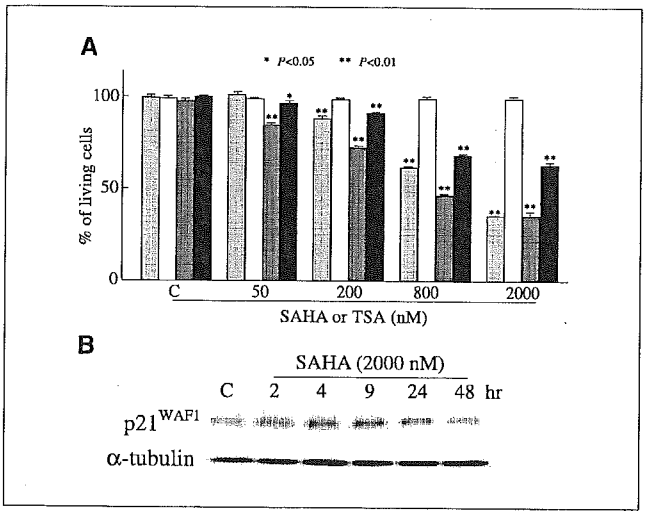

Figure 2. *A*, SAHA induced apoptosis in WB ras cells but not in HPMC. Cells were stained with FITC labeled Annexin V and propidium iodide after treatment with trichostatin-A or SAHA. The living cell population was defined as cells that were negative for both Annexin V and propidium iodide, being expressed as the percentage of cell numbers distributed in each quadrant. Results are means of at least three experiments; *P* values show significance levels compared with control (*C*). *Columns*, mean percentage of living cells in HPMC (*gray*, treated with trichostatin-A; *white*, SAHA) or WB-ras cells (*dark gray*, trichostatin-A; *black*, SAHA). *B*, SAHA induced $p21^{WAF1}$ protein in HPMC. HPMC was cultured with SAHA (2,000 nmol/L) for the indicated hours; *lane C*, untreated HPMC. Protein extracts (15 μg) were prepared and resolved on 15% SDS gels; $p21^{WAF1}$ protein was detected with the mouse monoclonal anti-$p21^{WAF1}$ antibody (F-5); the membrane was stripped and reprobed with α-tubulin as a loading control.

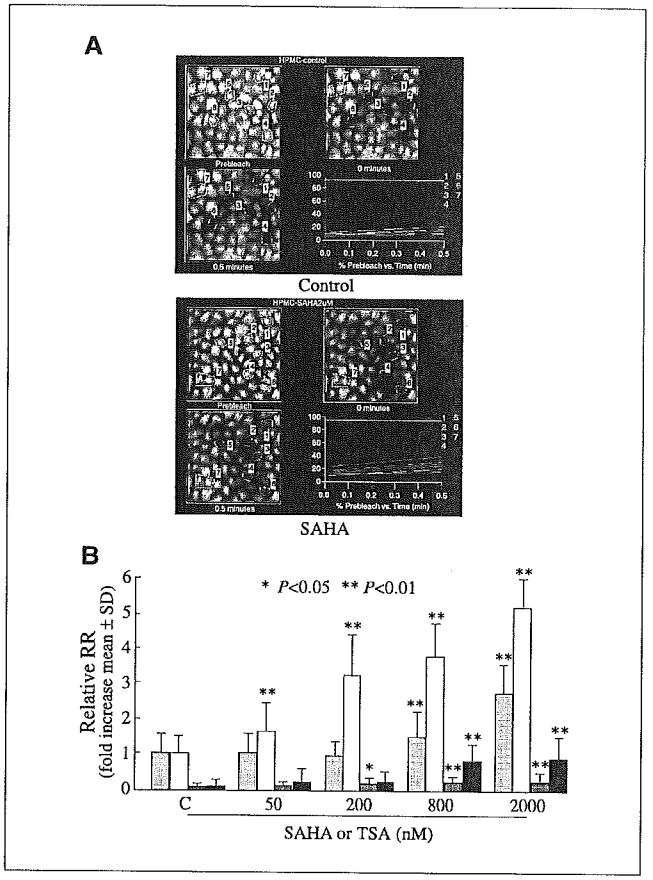

Figure 3. *A*, typical digitized fluorescence images on fluorescence recovery after photobleaching and plots of fluorescence recovery after photobleaching are shown. After culture with 2,000 nmol/L SAHA for 48 hours, HPMC was labeled with 5,6-carboxyfluorescein diacetate. Suitable fields of cells were identified using a ×40 objective lens. Each field was scanned to generate a digital image of fluorescence (Prebleach). After the initial scan, selected cells were photobleached (0 minute, *1-6*). Sequential scans were then carried out at 15-second intervals to detect the recovery of fluorescence in bleached cells (0.5 minute, *1-6*). Images were digitally recorded for analysis. Several unbleached cells were also monitored to provide control data (*7*). Typical plots of fluorescence recovery after photobleaching are shown (percentage prebleach versus time). An upward slope indicates the recovery of fluorescence. The percentage recovery of fluorescence over time was determined for each cell, and the data were corrected for background loss of fluorescence in one area (*7*). Untreated cells were used as the control. *B*, dose-course analyses of the effect of SAHA or trichostatin-A on gap junctional intercellular communication in HPMC. Gap junctional intercellular communication was estimated by fluorescence recovery after photobleaching assay in the cells cultured with SAHA or trichostatin-A. Results are expressed as the relative recovery rate (*RR*). The value from an untreated sample of HPMC (*C*, control) was taken as a unit to determine fold increase after culturing with SAHA or trichostatin-A (this scale is used for WB-ras cells for comparison). Results are means of at least three experiments; *P* values show significance levels compared with the control. *Columns*, relative recovery rate in the HPMC (*gray*, treated with trichostatin-A; *white*, SAHA) or WB-ras cells (*dark gray*, trichostatin-A; *black*, SAHA).

Suberoylanilide hydroxamic acid time and dose dependently accelerates acetylation of histones H3 and H4. We next determined the level of histone acetylation at each time point after culture with SAHA. Samples were collected from nuclear fractions of the cells cultured with SAHA (2,000 nmol/L) for 2, 4, 9, 24, and 48 hours, or with various concentrations (50, 200, 800, and 2,000 nmol/L) of SAHA for 48 hours. Western blot analysis showed that levels of acetylated histones H3 and H4 in untreated HPMC were low, and that accumulation of both acetylated histones

occurred at 2 hours after SAHA addition. This accumulation continued for 48 hours (Fig. 1*B1*). Incubation for 48 hours with SAHA resulted in accumulation of acetylated histones, which reached a peak at 800 nmol/L and was sustained at 2,000 nmol/L (Fig. 1*B1*). In contrast, histone H3 was weakly acetylated in untreated WB-ras cells. Treatment of WB-ras cells with SAHA resulted in accumulated acetylated histones H3 and H4, which reached a peak at 2,000 nmol/L (Fig. 1*B2*).

Suberoylanilide hydroxamic acid induces apoptosis in WB-ras cells, but not in human peritoneal mesothelial cells. Analyses of the cell cycle and apoptosis, using propidium iodide and Annexin V/propidium iodide, respectively, were done at 24 and 48 hours after culturing confluent cells with SAHA or trichostatin-A. SAHA exerted minimal effects on cell cycle progression in HPMC. Treatment for 24 hours with SAHA reduced the S-phase fraction (8.4% control versus 2.6% SAHA 2,000 nmol/L) but did not significantly alter the G_0-G_1 and G_2-M populations, whereas no subdiploid (apoptotic) population was detected. Treatment of HPMC with 50 to 2,000 nmol/L SAHA did not cause apoptotic cell death or reduce the living cell population in contrast to trichostatin-A, which dose-dependently induced apoptosis at >200 nmol/L. Both SAHA and trichostatin-A induced apoptotic cell death in WB-ras cells, although trichostatin-A showed greater potency (Fig. 2*A*).

Suberoylanilide hydroxamic acid induces transient expression of $p21^{WAF1}$. The effect of SAHA on $p21^{WAF1}$ protein levels was examined by Western blot analysis. HPMC was cultured with and without SAHA for 2, 4, 9, 24, and 48 hours. After culturing with SAHA, $p21^{WAF1}$ protein levels slightly increased at 2 hours, reached a peak at 9 hours, and decreased to control level after 48 hours treatment (Fig. 2*B*).

Suberoylanilide hydroxamic acid enhances gap junctional intercellular communication in human peritoneal mesothelial cell and WB-ras cells. Figure 3*A* shows typical digitized images obtained by the fluorescence recovery after photobleaching assay. After photobleaching, sequential scans detected the recovery of fluorescence in the bleached cells: The dye was transferred to photobleached cells through gap junctional intercellular communication from surrounding nonbleached cells. Recovery of fluorescence after photobleaching was much more rapid in HPMC cultured with SAHA (Fig. 3*A*, *SAHA*) than in untreated cells (Fig. 3*A*, *control*). SAHA was more efficient than trichostatin-A in enhancing the recovery rate in HPMC in a concentration-dependent manner. In WB-ras cells, both SAHA and trichostatin-A treatments also increased the recovery rate. Although their recovery levels were much lower, their enhancing rates relative to the control were no less than those in HPMC (Fig. 3*B*).

Suberoylanilide hydroxamic acid increases phosphorylated isoforms of Cx43. Western blotting was carried out to determine whether gap junctional intercellular communication activity was related to total Cx43 protein level and/or to the extent of Cx43 phosphorylation. Three forms of Cx43 immunoreactive protein (M_r 41,000-43,000) were observed in all samples in HPMC and nontransformed WB-F344 cells, as reported in previous papers (13, 14, 33, 34): A faster migrating band (P_0) and two slower migrating adjacent bands (two phosphorylated forms, P_1 and P_2;

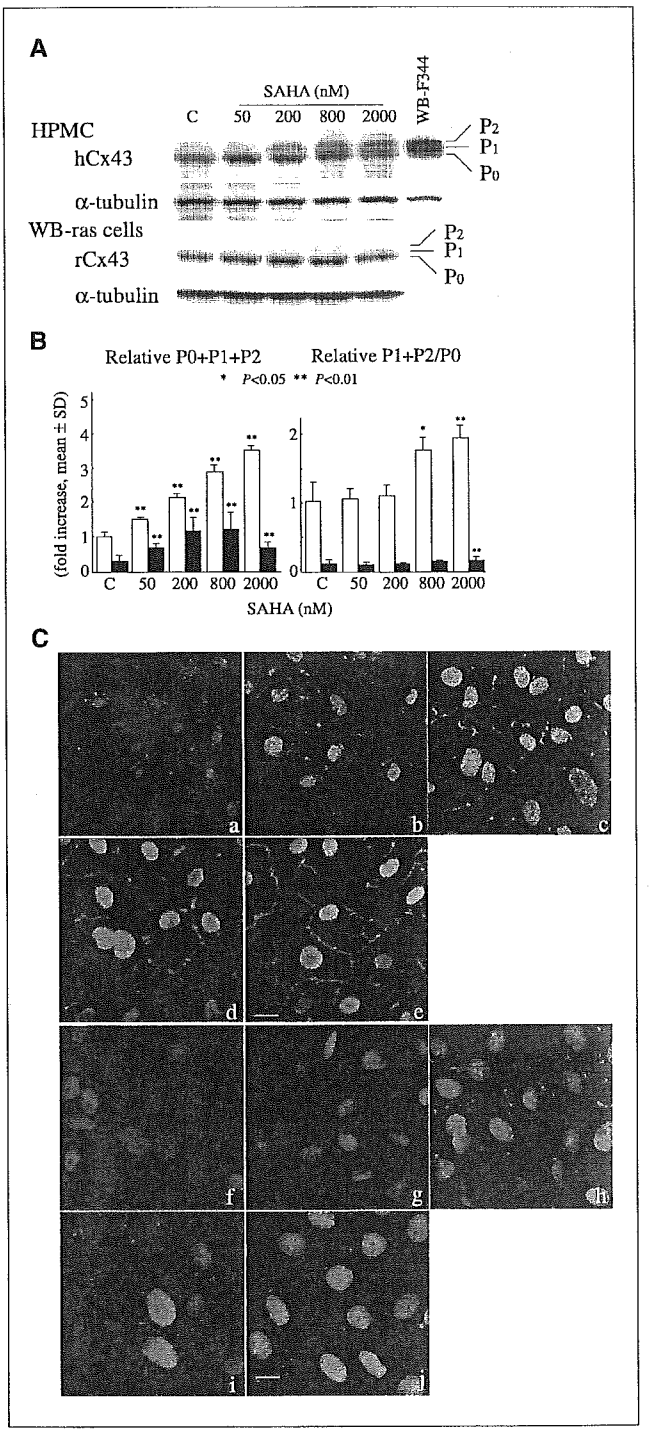

Figure 4. SAHA induced Cx43 protein in HPMC and WB-ras cells. HPMC and WB-ras cells were cultured with or without SAHA for 48 hours at indicated concentrations. *A*, Western blot analysis of Cx43 protein expression. Protein extracts from whole cells were prepared and resolved (30 μg) on 12.5% SDS/PAGE. Cx43 protein was detected by using mouse monoclonal antibody. WB-F344 (10 μg) cells were used as a positive control of Cx43 and the membrane was then stripped and reprobed with α-tubulin as a loading control. *B*, densitometric analysis of Cx43 protein bands in blotting membrane. The value from an untreated sample of HPMC (*C*, control) was taken as a unit to determine fold increase after culturing with SAHA. *Columns*, fold increase of Cx43 protein in HPMC (*white*) or WB-ras cells (*black*). *C*, intracellular localization of Cx43 and acetylated histone H3 protein was detected by immunofluorescence microscopy using monoclonal antibodies. *Red spots*, Cx43; *green spots*, acetylated histone H3. Images were acquired by confocal microscopy. HPMC: *a* to *e*, WB-ras cells; *f* to *j*, *a* (*f*), control; *b* (*g*), *c* (*h*), *d* (*i*), and *e* (*j*) with 50, 200, 800, 2,000 nmol/L SAHA, respectively. *Bars*, 20 μm (*a-e*); 10 μm (*f-j*).

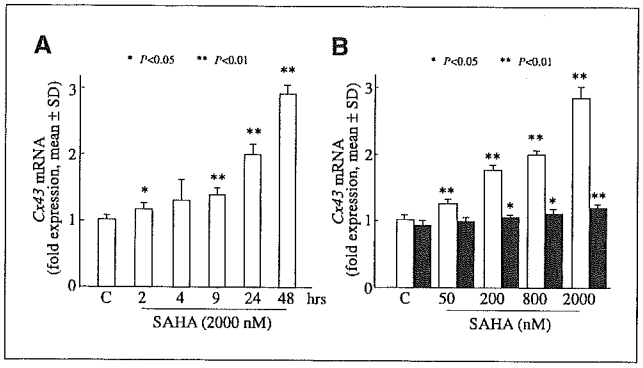

Figure 5. Real-time RT-PCR analysis of *Cx43* mRNA expression in HPMC and WB-ras cells. *A*, HPMC was cultured with 2,000 nmol/L SAHA for the indicated hours. *B*, HPMC and WB-ras cells were cultured with the indicated concentrations of SAHA for 48 hours. The value from untreated control of HPMC was taken as a unit to determine fold increase after culturing with SAHA. *Cx43* mRNA levels were normalized by *GAPDH* mRNA, whose levels did not change during culture with SAHA (data not shown). Results are means of at least three experiments: *P* values show significance levels compared with control (*C*). *Columns*, fold increase of *Cx43* mRNA in HPMC (*white*) or WB-ras cells (*black*).

Fig. 4*A*). Densitometric analysis of the results for HPMC showed that SAHA, at all concentrations, induced a significant dose-dependent increase in $P_1 + P_2$ (active form of Cx43) and $P_0 + P_1 + P_2$ (total Cx43), compared with control cells; the increase of P_0 with increased SAHA was less significant, compared with that of $P_1 + P_2$. As a result, $(P_1 + P_2) / P_0$ was increased by the treatment. In untreated WB-ras cells, P_0 was predominant, and the active forms $(P_1 + P_2)$ were minor. SAHA also induced an increase in active and total Cx43 protein in WB-ras cells, showing a peak at 800 nmol/L SAHA, although the ratio of $(P_1 + P_2) / P_0$ was very low compared with that in HPMC (Fig. 4*B*).

The localization of Cx43 protein and acetylated histone H3 was then examined by indirect immunofluorescence cytochemistry. Figure 4*C* shows immunostaining of the cells for Cx43 (*red*) and acetylated histone H3 (*green*) after 48-hour incubation with or without SAHA in HPMC (*a-e*) or WB-ras cells (*f-j*). The negative control, in which mouse or rabbit IgG was substituted for the primary antibodies, showed no staining (data not shown). Control cells showed that a few bright red spots (indicating Cx43 labeling) were dominant in cytoplasm rather than at the areas of intercellular contact. Incubation of HPMC with SAHA caused an increase in the number and size of the labeled regions, resulting in the cells displaying linear or dotted labeling along the membrane between cells, in contrast to control cells where a few positive spots were observed in cytoplasm. Although WB-ras cells showed altered immunostaining patterns in the same fashion as HPMC after treatment with SAHA, immunostaining was weaker for Cx43, displaying fewer spots in a nonlinear pattern along the membrane. The fluorescent levels of acetylated histone H3 seemed more prominent and concentrated in the nuclei in SAHA-treated HPMC and WB-ras cells compared with those in untreated cells.

Suberoylanilide hydroxamic acid induces a higher level of *Cx43* messenger RNA expression in human peritoneal mesothelial cell than in WB-ras cells. *Cx43* mRNA levels, measured by real-time RT-PCR, also increased in both HPMC and WB-ras cells cultured with SAHA in a time-dependent manner. *Cx43* mRNA in HPMC increased 3-fold over that of control cells after 48 hours culture with SAHA (Fig. 5*A*). Subsequently, we analyzed the *Cx43* mRNA levels, at various SAHA concentrations in HPMC as well as in WB-ras cells. *Cx43* mRNA levels in HPMC and WB-ras cells after 48 hours treatment with various concentrations of SAHA revealed dose-dependent increase of *Cx43* mRNA, which is much more remarkable in HPMC (3-fold increase at 2,000 nmol/L) than in WB-ras cells (1.3-fold increase at 2,000 nmol/L; Fig. 5*B*).

Suberoylanilide hydroxamic acid increases acetylated histones in chromatin fragments associated with *Cx43* gene. Chromatin immunoprecipitation analysis was used to study the mechanism of SAHA-induced expression of *Cx43*. Chromatin fragments from HPMC cultured with SAHA for 2 and 24 hours were immunoprecipitated with antibodies against acetylated histones H3 and H4. DNA from the immunoprecipitates was isolated, and real-time PCR, using *Cx43* primers, was done (Fig. 6*A*): The amounts of *Cx43* gene in acetylated histones H3 and H4 increased remarkably with increased hours of culture with SAHA (Fig. 6*B*). This observation confirms that histone acetylation is involved in the transcriptional regulation of *Cx43* expression, and that *Cx43* gene is a selective target for SAHA.

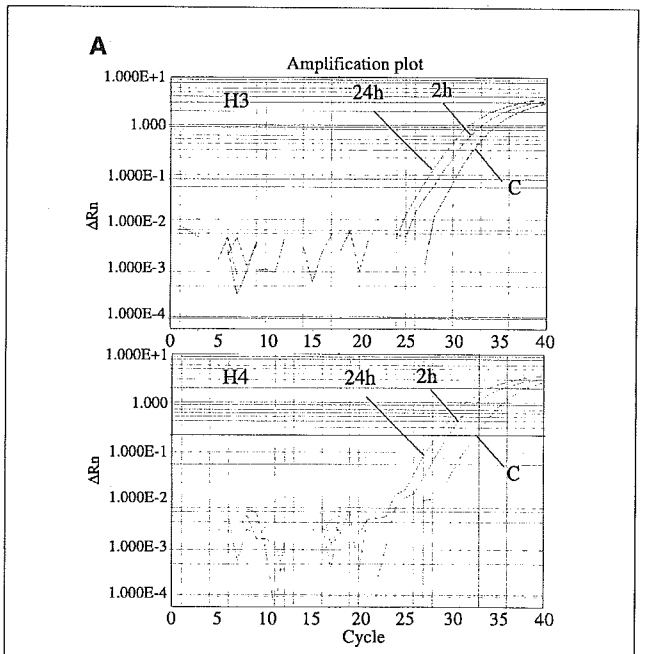

IP	SAHA (hrs)	Fold increase Mean	SD
Ac H3	C	1.00	0.04
	2	2.9	0.01
	24	6.9	0.10
Ac H4	C	1.00	0.03
	2	7.3	0.52
	24	16.8	1.01

Figure 6. SAHA-induced accumulation of acetylated histones H3 and H4 in the chromatin fragments associated with *Cx43* gene. Soluble chromatin from HPMC cultured with 2,000 nmol/L SAHA for 2 or 24 hours was immunoprecipitated with the antibodies against acetylated histone H3/H4. PCR primers used for *Cx43* mRNA were also used to amplify the DNA isolated from immunoprecipitated chromatin as described in Materials and Methods. *A*, the diagrams of real-time PCR analysis of the *Cx43* gene indicate that HPMC cultured with SAHA for 2 or 24 hours showed higher amplification levels when compared with untreated control cells. *B*, the relative amounts of DNA contained in acetylated histones were quantified by real-time PCR analysis. The value from an untreated control (*C*) was taken as a unit to determine fold increase.

Discussion

In this study, we showed that low concentrations (50-2,000 nmol/L) of SAHA enhanced gap junctional intercellular communication in normal HPMC via *Cx43* gene–associated histone acetylation without incurring apoptosis, whereas the same SAHA treatment of tumorigenic WB-ras cells induced apoptosis along with an increase of gap junctional intercellular communication. When we used WB-vector control cells (WB-neo), 50-2,000 nmol/L SAHA induced no apoptosis in these cells as it was the case in HPMC (data not shown), implying little difference in response to SAHA between rat and human nonmalignant cells. We also showed that SAHA-induced *Cx43* gene expression could be ascribed to histone H3/H4 acetylation. Our findings are the first demonstration of the efficacy of SAHA as an inhibitor of HDAC in nonmalignant cells to induce the transcriptional activation of the *Cx43* gene through histone acetylation. Furthermore, we showed that SAHA induced apoptosis in ras-transformed cells at a low concentration despite a smaller increase in *Cx43* mRNA and protein than in the case of HPMC.

Micromolar concentrations of SAHA have been shown to induce growth arrest and/or apoptosis in various transformed cells; the precise mechanism involved has been discussed with regard to variable transformed cells but not well defined (27, 35, 36). There seem to be two types of tumor cells based on their inability to have functional gap junctional intercellular communication: those whose connexin genes are not transcribed (37, 38) and those whose transcribed connexins have been rendered dysfunctional by a number of mechanisms, including posttranslational modification of connexin proteins by various activated oncogenes (18). Thus, one might expect to find differences in response to SAHA and trichostatin-A between normal cells that express connexins and tumor cells that express either very low levels of connexins or dysfunctional connexins. In confluent HPMC, nanomolar concentrations of SAHA generated a dose-dependent increase of *Cx43* mRNA and protein, whereas SAHA induced neither cell cycling arrest nor apoptosis. On the other hand, trichostatin-A induced apoptosis at a concentration (200 nmol/L) that did not increase recovery rate. Because we observed that histone H3 and H4 acetylation was also pronounced in cells treated with nanomolar SAHA, it seems unlikely that this difference mirrors the potency of the two HDAC inhibitors.

The cell cycle checkpoint gene $p21^{WAF1}$ was most commonly induced in various transformed cells cultured with SAHA (39) through histone acetylation (6, 40). In HPMC, $p21^{WAF1}$ level was elevated soon after the addition of SAHA and reverted to control level in 48 hours: This time course profile did not parallel the change in *Cx43* mRNA levels. Sodium butyrate, an HDAC inhibitor, has been shown to induce G_1 arrest and pRb dephosphorylation in 3T3 cells lacking $p21^{WAF1}$ (41). Richon et al. (6) found that the level of $p21^{WAF1}$ mRNA decreased within 24 hours after the addition of SAHA similar to our observation in HPMC. In contrast, chromatin immunoprecipitation analysis showed that *Cx43* gene-associated histone acetylation increased with increasing hours of culture with SAHA, similar to SAHA-induced expression of *Cx43* mRNA, indicating a more probable cause-effect between the two.

Differential response between HPMC and WB-ras cells was noted for SAHA-induced apoptosis, although histones H3/H4 acetylation was observed in both cells treated with nanomolar SAHA. Previous reports have shown that mitochondria played a central role during HDAC inhibitor–mediated apoptotic response (42–45). The cellular pathways via mitochondria and other apoptotic genes, targeted by SAHA, might differ between normal and malignant cells. Our results indicate that SAHA might suppress cancer cell growth through up-regulation of gap junctional intercellular communication, but does not cause damage in surrounding normal cells.

The role of SAHA in enhancing gap junctional intercellular communication in nonmalignant cells without serious adverse effects could be a beneficial for cancer prevention. Zhang et al. (46) recently reported that Cx43 displayed gap junction–independent growth inhibition of various tumor cells. Another connexin gene (i.e., *Cx26*) has been previously shown to be a tumor suppressor gene (47). Therefore, up-regulation of *Cx43* or other connexin genes could suppress tumor growth or progression by gap junction–dependent mechanism. Gap junctional intercellular communication is essential for maintaining homeostatic balance and normal differentiation through the modulation of cell growth and arrest. It will also be important to elucidate the role of histone acetylation and related proteins in the transcriptional regulation of *Cx43* and other connexin genes in selective tissues or cells. Future study will likely provide some answers to these questions.

Acknowledgments

Received 1/24/2005; revised 7/29/2005; accepted 8/19/2005.

Grant support: Baxter Limited Renal Division (T. Ogawa and T. Hayashi); Grants-in-Aid for Scientific Research from the Ministry of Education, Culture, Sports, Science and Technology of Japan; Ministry of Health and Welfare of Japan; Smoking Research Foundation (K. Nakachi); and National Institute of Environmental Health Sciences grant 5 P42 ES04911 (J.E. Trosko).

The costs of publication of this article were defrayed in part by the payment of page charges. This article must therefore be hereby marked *advertisement* in accordance with 18 U.S.C. Section 1734 solely to indicate this fact.

We thank Aton Pharma, Inc., a wholly owned subsidiary of Merck & Co., Inc., for providing SAHA.

References

1. Marks PA, Jiang X. Histone deacetylase inhibitors in programmed cell death and cancer therapy. Cell Cycle 2005;4:549–51.
2. Papeleu P, Vanhaecke T, Elaut G, et al. Differential effects of histone deacetylase inhibitors in tumor and normal cells—what is the toxicological relevance? Crit Rev Toxicol 2005;35:363–78.
3. Marks PA, Richon VM, Breslow R, Rifkind RA. Histone deacetylase inhibitors as new cancer drugs. Curr Opin Oncol 2001;13:477–83.
4. Melnick A, Licht JD. Histone deacetylases as therapeutic targets in hematologic malignancies. Curr Opin Hematol 2002;9:322–32.
5. Richon VM, Emiliani S, Verdin E, et al. A class of hybrid polar inducers of transformed cell differentiation inhibits histone deacetylases. Proc Natl Acad Sci U S A 1998;95:3003–7.
6. Richon VM, Sandhoff TW, Rifkind RA, Marks PA. Histone deacetylase inhibitor selectively induces p21WAF1 expression and gene-associated histone acetylation. Proc Natl Acad Sci U S A 2000;97:10014–9.
7. Butler LM, Agus DB, Scher HI, et al. Suberoylanilide hydroxamic acid, an inhibitor of histone deacetylase, suppresses the growth of prostate cancer cells *in vitro* and *in vivo*. Cancer Res 2000;60:5165–70.
8. Grunstein M. Histone acetylation in chromatin structure and transcription. Nature 1997;389:349–52.
9. Turner BM. Decoding the nucleosome. Cell 1993;75:5–8.
10. Van Lint C, Emiliani S, Verdin E. The expression of a small fraction of cellular genes is changed in response to histone hyperacetylation. Gene Expr 1996;5:245–53.
11. Sambucetti LC, Fischer DD, Zabludoff S, et al. Histone deacetylase inhibition selectively alters the activity and expression of cell cycle proteins leading to specific chromatin acetylation and antiproliferative effects. J Biol Chem 1999;274:34940–7.
12. Asklund T, Appelskog IB, Ammerpohl O, Ekstrom TJ, Almqvist PM. Histone deacetylase inhibitor 4-phenylbutyrate modulates glial fibrillary acidic protein and connexin 43 expression, and enhances gap-junction communication, in human glioblastoma cells. Eur J Cancer 2004;40:1073–81.
13. Ogawa T, Hayashi T, Kyoizumi S, Ito T, Trosko JE,

Yorioka N. Up-regulation of gap junctional intercellular communication by hexamethylene bisacetamide in cultured human peritoneal mesothelial cells. Lab Invest 1999;79:1511–20.
14. Ogawa T, Hayashi T, Yorioka N, Kyoizumi S, Trosko JE. Hexamethylene bisacetamide protects peritoneal mesothelial cells from glucose. Kidney Int 2001; 60:996–1008.
15. Andreeff M, Stone R, Michaeli J, et al. Hexamethylene bisacetamide in myelodysplastic syndrome and acute myelogenous leukemia: a phase II clinical trial with a differentiation-inducing agent. Blood 1992;80:2604–9.
16. Loewenstein WR. The cell-to-cell channel of gap junctions. Cell 1987;48:725–6.
17. Loewenstein WR. Junctional intercellular communication and the control of growth. Biochim Biophys Acta 1979;560:1–65.
18. Trosko JE, Ruch RJ. Cell-cell communication in carcinogenesis. Front Biosci 1998;3:208–36.
19. Yamasaki H, Naus CC. Role of connexin genes in growth control. Carcinogenesis 1996;17:1199–213.
20. Bruzzone R, White TW, Paul DL. Connections with connexins: the molecular basis of direct intercellular signaling. Eur J Biochem 1996;238:1–27.
21. Evans WH, Martin PE. Gap junctions: structure and function (review). Mol Membr Biol 2002;19:121–36.
22. Trosko JE, Chang CC, Madhukar BV, Klaunig JE. Chemical, oncogene and growth factor inhibition gap junctional intercellular communication: an integrative hypothesis of carcinogenesis. Pathobiology 1990;58: 265–78.
23. Klaunig JE, Ruch RJ. Role of inhibition of intercellular communication in carcinogenesis. Lab Invest 1990;62: 135–46.
24. Tsao MS, Smith JD, Nelson KG, Grisham JW. A diploid epithelial cell line from normal adult rat liver with phenotypic properties of "oval" cells. Exp Cell Res 1984;154:38–52.
25. De Feijter AW, Ray JS, Weghorst CM, et al. Infection of rat liver epithelial cells with v-Ha-ras: correlation between oncogene expression, gap junctional communication, and tumorigenicity. Mol Carcinog 1990;3:54–67.
26. Munster PN, Troso-Sandoval T, Rosen N, Rifkind R, Marks PA, Richon VM. The histone deacetylase inhibitor suberoylanilide hydroxamic acid induces differentiation of human breast cancer cells. Cancer Res 2001;61:8492–7.
27. Richon VM, Webb Y, Merger R, et al. Second generation hybrid polar compounds are potent inducers of transformed cell differentiation. Proc Natl Acad Sci U S A 1996;93:5705–8.
28. Leoni F, Zaliani A, Bertolini G, et al. The antitumor histone deacetylase inhibitor suberoylanilide hydroxamic acid exhibits antiinflammatory properties via suppression of cytokines. Proc Natl Acad Sci U S A 2002; 99:2995–3000.
29. Ishiyama M, Tominaga H, Shiga M, Sasamoto K, Ohkura Y, Ueno K. A combined assay of cell viability and *in vitro* cytotoxicity with a highly water-soluble tetrazolium salt, neutral red and crystal violet. Biol Pharm Bull 1996;19:1518–20.
30. Trosko JE, Chang CC, Wilson MR, Upham B, Hayashi T, Wade M. Gap junctions and the regulation of cellular functions of stem cells during development and differentiation. Methods 2000;20:245–64.
31. Wade MH, Trosko JE, Schindler M. A fluorescence photobleaching assay of gap junction-mediated communication between human cells. Science 1986;232: 525–8.
32. Luo RX, Postigo AA, Dean DC. Rb interacts with histone deacetylase to repress transcription. Cell 1998; 92:463–73.
33. de Feijter AW, Matesic DF, Ruch RJ, Guan X, Chang CC, Trosko JE. Localization and function of the connexin 43 gap-junction protein in normal and various oncogene-expressing rat liver epithelial cells. Mol Carcinog 1996;16:203–12.
34. Esinduy CB, Chang CC, Trosko JE, Ruch RJ. *In vitro* growth inhibition of neoplastically transformed cells by non-transformed cells: requirement for gap junctional intercellular communication. Carcinogenesis 1995;16: 915–21.
35. Chen H, Lin RJ, Xie W, Wilpitz D, Evans RM. Regulation of hormone-induced histone hyperacetylation and gene activation via acetylation of an acetylase. Cell 1999;98:675–86.
36. Vrana JA, Decker RH, Johnson CR, et al. Induction of apoptosis in U937 human leukemia cells by suberoylanilide hydroxamic acid (SAHA) proceeds through pathways that are regulated by Bcl-2/Bcl-XL, c-Jun, and p21CIP1, but independent of p53. Oncogene 1999;18:7016–25.
37. Momiyama M, Omori Y, Ishizaki Y, et al. Connexin26-mediated gap junctional communication reverses the malignant phenotype of MCF-7 breast cancer cells. Cancer Sci 2003;94:501–7.
38. King TJ, Fukushima LH, Donlon TA, Hieber AD, Shimabukuro KA, Bertram JS. Correlation between growth control, neoplastic potential and endogenous connexin43 expression in HeLa cell lines: implications for tumor progression. Carcinogenesis 2000;21: 311–5.
39. Marks PA. The mechanism of the anti-tumor activity of the histone deacetylase inhibitor, suberoylanilide hydroxamic acid (SAHA). Cell Cycle 2004;3:534–5.
40. Bunz F, Dutriaux A, Lengauer C, et al. Requirement for p53 and p21 to sustain G_2 arrest after DNA damage. Science 1998;282:1497–501.
41. Vaziri C, Stice L, Faller DV. Butyrate-induced G_1 arrest results from p21-independent disruption of retinoblastoma protein-mediated signals. Cell Growth Differ 1998;9:465–74.
42. Zhu WG, Lakshmanan RR, Beal MD, Otterson GA. DNA methyltransferase inhibition enhances apoptosis induced by histone deacetylase inhibitors. Cancer Res 2001;61:1327–33.
43. Ruefli AA, Ausserlechner MJ, Bernhard D, et al. The histone deacetylase inhibitor and chemotherapeutic agent suberoylanilide hydroxamic acid (SAHA) induces a cell-death pathway characterized by cleavage of Bid and production of reactive oxygen species. Proc Natl Acad Sci U S A 2001;98:10833–8.
44. Medina V, Edmonds B, Young GP, James R, Appleton S, Zalewski PD. Induction of caspase-3 protease activity and apoptosis by butyrate and trichostatin A (inhibitors of histone deacetylase): dependence on protein synthesis and synergy with a mitochondrial/cytochrome *c*-dependent pathway. Cancer Res 1997;57:3697–707.
45. Herold C, Ganslmayer M, Ocker M, et al. The histone-deacetylase inhibitor trichostatin A blocks proliferation and triggers apoptotic programs in hepatoma cells. J Hepatol 2002;36:233–40.
46. Zhang YW, Kaneda M, Morita I. The gap junction-independent tumor-suppressing effect of connexin 43. J Biol Chem 2003;278:44852–6.
47. Lee SW, Tomasetto C, Sager R. Positive selection of candidate tumor-suppressor genes by subtractive hybridization. Proc Natl Acad Sci U S A 1991;88:2825–9.

SHORT REPORT

Cytogenetic differences in breast cancer samples between German and Japanese patients

J Packeisen, K Nakachi, W Boecker, B Brandt, H Buerger

J Clin Pathol 2005;**58**:1101–1103. doi: 10.1136/jcp.2004.022392

Background: Japanese and German breast cancer cases differ substantially in the frequency of *egfr* amplification.
Aims: To unravel further the cytogenetic differences between Japanese and German breast cancer cases.
Methods: Forty one Japanese breast cancer cases were evaluated by means of comparative genomic hybridisation (CGH). The results were compared with the CGH results from 161 German breast cancer cases.
Results: The mean number of genetic alterations/case was significantly higher in German premenopausal patients with breast cancer than in their Japanese counterparts. Japanese breast cancer cases revealed a higher number of chromosome 17p losses. Losses of 8p were associated with oestrogen receptor (ER) negativity in Japanese patients with breast cancer, whereas in the German patients gains of 3q and 6q were associated with the lack of ER expression.
Conclusions: The interethnic differences of invasive breast cancer are reflected by cytogenetic aberrations, which are also associated with the differential expression of the ER.

Substantial epidemiological and clinical differences have been reported between Japanese and white patients with breast cancer.[1] Most cytogenetic studies published so far, using comparative genomic hybridisation (CGH) as a screening technique for the detection of unbalanced cytogenetic alterations within a given tumour, have concentrated on white women.[2–4] In contrast, little is known about the cytogenetic aberrations in breast cancer in patients of Asian origin.[5]

Significant differences are known to exist between white and Asian populations for many polymorphic DNA sequences. A study published by our group previously identified a polymorphic sequence in intron 1 of the epidermal growth factor receptor (EGFR) gene (*egfr*) that had a significantly longer CA repeat stretch in Japanese than in German women. In vitro and in vivo experiments showed that the longer CA repeat stretch in Japanese patients was associated with a higher frequency of *egfr* gene amplification[6] and EGFR expression. Therefore, it is possible that other polymorphic sites exist that have distinct chromosomal aberrations in the different ethnic subgroups.

> "Significant differences are known to exist between white and Asian populations for many polymorphic DNA sequences"

MATERIAL AND METHODS

Forty one cases of Japanese breast cancer were analysed by CGH and these results were compared with those from 161 invasive breast tumours from German women, originating from the files of the Gerhard-Domagk Institute of Pathology. None of the patients had preoperative treatment. Table 1 provides further details of the investigated tumour samples. The Japanese breast cancer cases originated from the files of the Saitama Cancer Centre Hospital, Japan. The method of CGH analysis, the criteria for the evaluation of genetic alterations, and the immunohistochemical evaluation of the steroid receptor content were performed as described previously.[7]

Statistical tests

Statistics were performed using Fisher's exact test and the Mann-Whitney U test. p Values were two tailed and not adjusted for multiple comparisons; p values < 0.05 were considered significant.

RESULTS

In accordance with the literature, 28 of 41 (68%) of the Japanese and 51 of 161 (32%) of the German patients with breast cancer were premenopausal. The mean age was 51.9 (SD, 13.1) and 59.9 (SD, 15.0) years in Japanese and German patients with breast cancer, respectively ($p < 0.01$). Table 1 provides a detailed characterisation of the patients. Table 2 provides an overview of the most common quantitative cytogenetic aberrations.

A detailed characterisation of the German patients with breast cancer has been published previously.[7 8] On average, the German breast cancer cases revealed 8.5 alterations/case (9.6 and 8.1 in premenopausal and postmenopausal patients, respectively), whereas the Japanese patients with breast cancer had a significantly lower average number of alterations/case (7.2; 6.3 and 8.7 in premenopausal and postmenopausal patients, respectively; $p < 0.05$). ER positive cases had a lower average number of alterations/case compared with ER negative tumours in both subgroups (7.5 *v* 10.5 ($p < 0.01$) in German and 6.2 *v* 8.7 ($p = 0.11$) in Japanese patients with breast cancer). ER negative tumours showed a similar frequency of aberrations irrespective of menopausal status in German patients, whereas postmenopausal Japanese patients with ER negative tumours showed a clear increase in cytogenetic alterations. The Japanese ER positive subgroup showed a higher rate of 16q losses, whereas ER negative cases showed an increased rate of 8p losses ($p < 0.05$ for both parameters). German ER positive tumours also had a significantly increased rate of 16q losses ($p < 0.05$) and a decreased rate of 3q ($p < 0.01$) and 6q gains ($p < 0.05$).

The recurrent changes seen most frequently in German and Japanese breast cancer cases were gains of 1q, 3q, 6q, 8q, 17q, and 20q in addition to losses of 6q, 8p, 11q, 13q, and 16q. 17p losses were predominantly seen in Japanese patients with breast cancer ($p < 0.001$).

Abbreviations: CGH, comparative genomic hybridisation; EGFR, epidermal growth factor receptor; ER, oestrogen receptor

Table 1 Overview of the distribution of clinicopathological parameters in both patient cohorts

Characteristic	Japanese n=41	German n=161
Menopausal status		
Premenopausal	28 (68%)	51 (32%)
Postmenopausal	13 (32%)	110 (68%)
Stage		
I	14 (35%)	51 (32%)
IIa	11 (27%)	40 (25%)
IIb	5 (11%)	24 (15%)
IIIa	4 (10%)	18 (11%)
IIIb	4 (10%)	20 (12%)
IV	3 (7%)	8 (5%)
Grade		
I	8 (19%)	18 (11%)
II	18 (44%)	77 (48%)
III	15 (37%)	66 (41%)
Tumour type		
Ductal invasive	36 (87%)	121 (75%)
Lobular invasive	5 (13%)	25 (16%)
Miscellaneous subtypes		15 (9%)
Oestrogen receptor status		
Negative	18 (43%)	65 (40%)
Positive	23 (57%)	96 (60%)

Table 2 Summary of cytogenetic alterations in the Japanese and German breast cancer subgroups

	Germany	Japan	p Value
Mean number of cytogenetic alterations/case			
All	8.5	7.2	
Premenopausal	9.6	6.3	p<0.05
Postmenopausal	8.1	8.7	
ER+	7.5	6.2	
ER−	10.5	8.7	
	p<0.01	p=0.11	
Frequency of the most recurrent cytogenetic alterations			
1q gains	70%	78%	NS
3q gains	23%	11%	NS
6q gains	11%	14%	NS
8q gains	49%	46%	NS
17q gains	18%	26%	NS
20q gains	20%	17%	NS
6q losses	21%	19%	NS
8p losses	34%	26%	NS
13q losses	26%	19%	NS
16q losses	53%	39%	NS
17p losses	22%	63%	p<0.001
Frequency of the most common chromosomal high level gains			
8q	18%	21%	NS
11q	10%	7%	NS
17q	18%	12%	NS
20q	6%	5%	NS

The rate and distribution of high level gains, indicative of gene amplification, was similar in both ethnic subgroups (36% in German patients compared with 44% in the Japanese ones).

Other than the above described correlations between cytogenetic alterations and clinicopathological parameters, no distinct cytogenetic alterations were found in Japanese patients with breast cancer.

DISCUSSION

Recently, significant differences have been shown in relation to the length of a polymorphic sequence within the intron 1 of *egfr*, the frequency of *egfr* mutations, and the expression of EGFR between Japanese and German patients with breast cancer.[6] Interestingly, similar differences have also been described for activating mutations of *egfr* in Japanese and white patients with lung cancer.[10]

The idea of different genotypes leading to a similar phenotype led us to the comparative cytogenetic analysis of Japanese and German patients with breast cancer. In addition to the differences in *egfr* amplification previously described in this series, a significantly higher incidence of 17p losses was found in Japanese breast cancer cases compared with German breast cancer cases. The frequency of 17p losses was even higher than that seen in German ductal invasive G3 carcinomas, which generally display the highest frequency of 17p losses.[3 4 11] This feature was not affected by menopausal or ER status, and these results are still open to interpretation. The role of p53 (with its chromosomal locus at 17p13.1) in this scenario remains unclear, because p53 mutations are associated with worse prognosis and a lower degree of histopathological differentiation, features less common in Japanese breast cancer.[12] Alternatively, another putative tumour suppressor gene within 17p13 might contribute to breast carcinogenesis predominantly in Japanese patients with breast cancer[13 14]; however, alterations within this suspected tumour suppressor gene appear to be associated with highly proliferative breast cancers with a poor prognosis,[15] which again is contradictory to the tumour biological features seen in Japanese patients with breast cancer in general and also in our series.

A higher average number of cytogenetic alterations/case correlates with an increased recurrence rate in node negative breast cancer, and therefore with overall prognosis.[16] In accordance with this, there was a slightly increased average number of genetic alterations in all German breast cancer cases and a decreased number of genetic alterations in German postmenopausal breast cancer cases. Interestingly, there was a significantly higher average number of genetic alterations/case in the German premenopausal patients with breast cancer than in their Japanese counterparts.

> "It is interesting that, irrespective of menopausal status, our German patients with oestrogen receptor (ER) negative cancer had a significantly higher average number of cytogenetic alterations/case compared with ER positive patients"

The regulation of ER expression between Japanese and German patients with breast cancer is similar in some respects but different in others. Different levels of ER expression in benign breast tissue between Japanese and white populations have been reported as an underlying cause of differences in breast cancer incidence between these two populations. The exact reasons for this observation are unclear, although the influence of food habits has been discussed.[17] A higher rate of ER negativity has been found in Japanese postmenopausal patients with breast cancer compared with matched white patients, and this correlated with a worse prognosis in the Japanese patients.[18] It is interesting that, irrespective of menopausal status, our German patients with ER negative cancer had a significantly higher average number of cytogenetic alterations/patient ($p < 0.01$) compared with ER positive patients. This was also true for our Japanese patients with breast cancer, with the exception of premenopausal patients, in whom no quantitative cytogenetic impact of ER expression could be measured.

However, similar cytogenetic alterations associated with the regulation of ER expression appear to be present in German and Japanese patients with breast cancer. This is especially true for chromosomal 16q losses in ER positive carcinomas in both ethnic groups, as described previously.[11 19] Our series did not reveal the biological importance of 8p

Take home messages

- The average number of genetic alterations/case was significantly higher in German premenopausal patients with breast cancer than in their Japanese counterparts
- There were a higher number of chromosome 17p losses in Japanese patients
- Losses of 8p were associated with oestrogen receptor (ER) negativity in Japanese patients with breast cancer, whereas in the German patients gains of 3q and 6q were associated with the lack of ER expression
- Thus, the interethnic differences of invasive breast cancer are reflected by cytogenetic aberrations, which are also associated with differential expression of ER

losses associated with ER negativity in the German breast cancer cases. Losses at this site were found in all but one CGH study on white patients with breast cancer.[19 20] The number of Japanese tumours investigated in our series might be too small to draw definite conclusions concerning 3q and 6q gains in Japanese patients with breast cancer because these changes are relatively rare events in breast cancer. Gains of 3q and 6q have been shown to be associated with an increased level of telomerase activity, cytogenetic instability, and tumour proliferation, suggesting an interplay between these parameters.[21]

In summary, our results show that there are cytogenetic differences between Japanese and German breast cancer cases. Further studies are needed to define the extent to which these differences are causative or merely a reflection of other underlying genetic disturbances that are not detectable by means of CGH.

Authors' affiliations
J Packeisen, Institute of Pathology, 49076 Osnabrück, Germany
K Nakachi, Department of Epidemiology, Saitama Cancer Centre, Saitama 362-0806 Japan
W Boecker, H Buerger, Institute of Pathology, University of Muenster, 48149 Muenster, Germany
B Brandt, Institute of Clinical Chemistry and Laboratory Medicine, University of Muenster

Correspondence to: Professor H Buerger, Institute of Pathology, Westfälische Wilhelmsuniversität Münster, Domagkstr. 173, 48149 Münster, Germany; burgerh@uni-muenster.de

Accepted for publication 18 February 2005

REFERENCES

1 **Sakamoto G**, Sugano H. Pathology of breast cancer: present and prospect in Japan. *Breast Cancer Res Treat* 1991;**18**(suppl 1):S81–3.
2 **Ried T**, Just KE, Holtgreve Grez H, *et al.* Comparative genomic hybridization of formalin-fixed, paraffin-embedded breast tumours reveals different patterns of chromosomal gains and losses in fibroadenomas and diploid and aneuploid carcinomas. *Cancer Res* 1995;**55**:5415–23.
3 **Buerger H**, Otterbach F, Simon R, *et al.* Different genetic pathways in the evolution of invasive breast cancer are associated with distinct morphological subtypes. *J Pathol* 1999;**189**:521–6.
4 **Roylance R**, Gorman P, Harris W, *et al.* Comparative genomic hybridization of breast tumours stratified by histological grade reveals new insights into the biological progression of breast cancer. *Cancer Res* 1999;**59**:1433–6.
5 **Fung LF**, Wong N, Tang N, *et al.* Genetic imbalances in pT2 breast cancers of southern Chinese women. *Cancer Genet Cytogenet* 2001;**124**:56–61.
6 **Buerger H**, Packeisen J, Boecker A, *et al.* Allelic length of a CA dinucleotide repeat in the egfr gene correlates with the frequency of amplifications of this sequence—first results of an inter-ethnic breast cancer study. *J Pathol* 2004;**203**:545–50.
7 **Buerger H**, Mommers E, Littmann R, *et al.* Ductal invasive G2 and G3 carcinomas of the breast are the end stages of at least two different lines of genetic evolution. *J Pathol* 2001;**194**:165–70.
8 **Agelopoulos K**, Tidow N, Korsching E, *et al.* Molecular cytogenetic investigations of synchronous bilateral breast cancer. *J Clin Pathol* 2003;**56**:660–5.
9 **Buerger H**, Simon R, Schaefer KL, *et al.* Genetic relationship of lobular carcinoma in situ, ductal carcinoma in situ and associated invasive carcinoma of the breast. *Mol Pathol* 2000;**53**:118–21.
10 **Paez JG**, Janne PA, Lee JC, *et al.* EGFR mutations in lung cancer: correlation with clinical response to gefitinib therapy. *Science* 2004;**304**:1497–500.
11 **Tirkkonen M**, Tanner M, Karhu R, *et al.* Molecular cytogenetics of primary breast cancer by CGH. *Genes Chromosomes Cancer* 1998;**21**:177–84.
12 **Higuchi CM**, Serxner SA, Nomura AM, *et al.* Histopathological predictors of breast cancer death among Caucasians and Japanese in Hawaii. *Cancer Epidemiol Biomarkers Prev* 1993;**2**:201–5.
13 **Coles C**, Thompson AM, Elder PA, *et al.* Evidence implicating at least two genes on chromosome 17p in breast carcinogenesis. *Lancet* 1990;**336**:761–3.
14 **Cornelis RS**, van Vliet M, Vos CB, *et al.* Evidence for a gene on 17p13.3, distal to TP53, as a target for allele loss in breast tumors without p53 mutations. *Cancer Res* 1994;**54**:4200–6.
15 **Merlo GR**, Venesio T, Bernardi A, *et al.* Loss of heterozygosity on chromosome 17p13 in breast carcinomas identifies tumors with high proliferation index. *Am J Pathol* 1992;**140**:215–23.
16 **Isola JJ**, Kallioniemi OP, Chu LW, *et al.* Genetic aberrations detected by comparative genomic hybridization predict outcome in node-negative breast cancer. *Am J Pathol* 1995;**147**:905–11.
17 **Lawson JS**, Field AS, Champion S, *et al.* Low oestrogen receptor alpha expression in normal breast tissue underlies low breast cancer incidence in Japan [letter]. *Lancet* 1999;**354**:1787–8.
18 **Stemmermann GN.** The pathology of breast cancer in Japanese women compared to other ethnic groups: a review. *Breast Cancer Res Treat* 1991;**18**(suppl 1):S67–72.
19 **Richard F**, Pacyna Gengelbach M, Schl Fleige B, *et al.* Patterns of chromosomal imbalances in invasive breast cancer. *Int J Cancer* 2000;**89**:305–10.
20 **Rennstam K**, Ahlstedt-Soini M, Baldetorp B, *et al.* Patterns of chromosomal imbalances defines subgroups of breast cancer with distinct clinical features and prognosis. A study of 305 tumors by comparative genomic hybridization. *Cancer Res* 2003;**63**:8861–8.
21 **Loveday RL**, Greenman J, Drew PJ, *et al.* Genetic changes associated with telomerase activity in breast cancer. *Int J Cancer* 1999;**84**:516–20.

Supplement to Journal of Epidemiology Volume 15 (Supplement I) March 2005

Stability of Frozen Serum Levels of Insulin-like Growth Factor-Ⅰ, Insulin-like Growth Factor-Ⅱ, Insulin-like Growth Factor Binding Protein-3, Transforming Growth Factor β, Soluble Fas, and Superoxide Dismutase Activity for the JACC Study

Yoshinori Ito, Kei Nakachi, Kazue Imai, Shuji Hashimoto, Yoshiyuki Watanabe, Yutaka Inaba, Akiko Tamakoshi, Takesumi Yoshimura, for the JACC Study Group.

Stability of Frozen Serum Levels of Insulin-like Growth Factor-I, Insulin-like Growth Factor-II, Insulin-like Growth Factor Binding Protein-3, Transforming Growth Factor β, Soluble Fas, and Superoxide Dismutase Activity for the JACC Study

Yoshinori Ito,[1] Kei Nakachi,[2] Kazue Imai,[2] Shuji Hashimoto,[3] Yoshiyuki Watanabe,[4] Yutaka Inaba,[5] Akiko Tamakoshi,[6] Takesumi Yoshimura,[7] for the JACC Study Group.

BACKGROUND: Subjects of the Japan Collaborate Cohort Study (JACC Study) gave peripheral blood samples collected between 1988 and 1990. We conducted to investigate whether levels of serum components measured after 9 years of frozen storage are stable or not.
METHODS: To assess the degradation of frozen serum components in the JACC Study, we compared levels of various components (IGF-I, IGF-II, IGFBP-3, TGF-β1, sFas, and total SOD activity) between fresh and stored sera collected from other inhabitants. Serum levels of constituents were measured by immunoradiometric assay (IGF-I, IGF-II and IGFBP-3), quantitative enzyme immunoassay (TGF-β1), enzyme-linked immuno-adsorbent assay (sFas), and an improved nitrite method (SOD activity).
RESULTS: The coefficients of variation for intra- and inter-assay precisions of the measurements were less than 9%. Levels of IGF-I, IGF-II, IGFBP-3, TGF-β1 and sFas in sera after storage for 9 years at -80℃ were similar to those of fresh sera newly collected from inhabitants. The distributions of serum IGF-I, IGF-II, IGFBP-3, TGF-β1, sFas and SOD activity for specimens collected from different individuals tended to be similar to those of serum levels for frozen specimens collected from different individuals and stored for 9 years.
CONCLUSIONS: There was no statistically significant difference in distribution of measured values of IGF-I, IGF-II, IGFBP-3, TGF-β1, and sFas between newly collected sera and frozen specimens stored for 9 years. Thus, measurements of these serum constituents of specimens stored for the JACC Study can be reliably used in nested case-control study.
J Epidemiol 2005;15:S67-S73.

Key words: Serum Storage, IGFs, sFas, TGF-β, SOD

The Japan Collaborate Cohort Study for Evaluation of Cancer Risk (JACC Study), sponsored by Monbusho (the Ministry of Education, Science, Sports and Culture of Japan), involves more than 127,477 participants living in 45 municipalities all over Japan.[1,2] Subjects of the JACC Study completed a survey and gave peripheral blood samples collected from 39,242 registered subjects (aged from 40 to 79 years) between 1988 and 1990. Serum from these samples was separated from blood cells and stored in deep freezers at -80℃ until 1999; serum of each participant was divided into 3 to 5 tubes (100 to 500 μL per tube). These serum

Received September 17, 2004, and accepted December 19, 2004.
The JACC Study has been supported by Grants-in-Aid for Scientific Research from the Ministry of Education, Science, Sports and Culture of Japan (Monbusho) (No. 61010076, 62010074, 63010074, 1010068, 2151065, 3151064, 4151063, 5151069, 6279102 and 11181101).

[1] Department of Public Health, Fujita Health University School of Health Sciences.
[2] Department of Radiobiology/Molecular Epidemiology, Radiation Effects Research Foundation.
[3] Department of Hygiene, Fujita Health University School of Medicine.
[4] Department of Epidemiology for Community Health and Medicine, Kyoto Prefecture University of Medicine Graduate School of Medical Science.
[5] Department of Epidemiology and Environmental Health, Juntendo University School of Medicine.
[6] Department of Preventive Medicine/Biostatistics and Medical Decision Making, Nagoya University Graduate School of Medicine.
[7] Fukuoka Institute of Health and Environmental Sciences.
Address for correspondence: Yoshinori Ito, Department of Public Health, Fujita Health University School of Health Sciences, 1-98 Dengakugakubo, Kutsukake-cho, Toyoake City, Aichi Prefecture 470-1192, Japan. (yoshiito@fujita-hu.ac.jp)

samples are used to study the relation between serum component levels and the incidence or mortality of cancer or other diseases.

Recently, cancer prevention research has focused on molecular biology related to genes, cytokines and special molecules associated with the promotion or inhibition of the development of carcinogenesis and apoptosis. There were some reports of the relationship investigated between cancer and the following serum constituents: insulin-like growth factor (IGF)-I, IGF-II,[3-5] insulin-like growth factor-binding protein 3 (IGFBP-3),[6] transforming growth factor (TGF)-β 1,[7,8] soluble Fas (sFas),[9] and superoxide dismutase (SOD) activity.[10-13] Although reports indicate that serum levels of constituents such as proteins and minerals are stable in long-term refrigerated storage,[14-17] there have been no reports indicating whether serum levels of cytokines, such as IGFs, TGF-β and sFas, remain stable after approximately 10 years of storage at -80℃.

In the present study, we examined whether cytokines and other constituents in frozen sera remained stable during long-term storage at -80℃, using stored and fresh serum samples separately collected from other subjects.

METHODS

Serum Samples

Approximately 2 liters of pooled sera prepared to evaluate the stability of serum biochemical constituents for the JACC Study was collected from individuals who participated in health check-up programs for workers in certain industries. After centrifugation and filtration 3 times, 1mL samples of the pooled sera were put into 2-ml cups that were sealed with a polypropylene stopper, distributed to laboratories and stored at -80℃ beginning in 1988. Fresh sera used for comparison of serum levels between fresh and frozen sera were separately collected from inhabitants of rural Saitama (1999) and Hokkaido (1990) who participated in health check-up programs. Serum samples used for comparison of serum level of inhabitants, aged 40 to 80, were collected from residents of Hokkaido who attended health check-up programs in August 1991 and 1999. Approximately 3mL serum samples were poured into polypropylene cups sealed with a polypropylene stopper, and were stored at -80℃ until the time of measurement of components. Reference sera for intra- and inter-assay precisions were used different levels of controlled specimens or pooled sera specially prepared by SRL Laboratory (SRL Laboratory, Hachioji).

Measurements of serum constituents

We measured serum levels of IGF-I, IGF-II, IGFBP-3, TGF-β 1, sFas and total SOD activity. All measurements were performed using the same batched-reagent set, by trained staff at a single laboratory (SRL Laboratory, Hachioji). Measurements used for comparison between fresh and stored sera were performed in 1999. Serum component levels of pooled sera were measured using a SMAC auto-analyzer (Technicon Co., Ltd.; for measurements in 1988) and a TBA auto-analyzer (Toshiba K.K.; for measurements in 1994).

Serum levels of IGF-I, IGF-II and IGFBP-3 were measured by immuno-radiometric assay, using commercially available kits (Daiichi Radioisotope Lab., Tokyo)[18-20] (Table 1). Serum TGF-β 1 was measured by quantitative sandwich enzyme immunoassay (ELISA), using commercially available kits (R&D Systems Inc., Minneapolis).[21,22] Serum sFas was assayed by enzyme-linked immuno-adsorbent assay (ELISA), using commercially available kits (MBL Co., Ltd., Nagoya).[23,24] Serum SOD activity was estimated from the decreasing rate of nitrite produced by hydroxylamine and superoxide anions, based on an improved nitrite method.[25]

The coefficients of variation (CV) of intra- and inter-assay precisions for each determination were calculated: from 10 determinations of 3 different reference sera for intra-assay precision; and from 5-day determinations of 5 different reference sera for inter-assay precision. Each range of CV values estimated with different reference sera was presented as the lowest and highest mean values. The ranges of inter-assay precision for the JACC Study were represented as the low and high CV values calculated from the reference serum levels estimated in each assay of the JACC Study samples. Paired t-tests were performed to evaluate the mean differences between fresh and frozen sample levels.

Our entire study design, which comprised singular and collective use of epidemiological data and sera, was approved by the Ethical Board at Nagoya University School of Medicine, where the central secretariat of the JACC study is located.

RESULTS

The range of the assays for reliable measurement of IGF-I, IGF-II and IGFBP-3 in reference sera was 4 to 2,000 ng/mL, 10 to 1,640 ng/mL, and 0.06 to 10.10 μ g/mL, respectively (Table 1). The intra- and inter-assay precisions obtained using different reference sera for each determination method was as follows: for the IGF-I assay, 2.15 to 3.53% and 1.12 to 4.18% of the CV values, respectively; for the IGF-II assay, 2.74 to 4.45% and 4.23 to 5.53%; for the IGFBP-3 assay, 3.16 to 4.19% and 5.28 to 8.89%. The range of the assay for serum TGF-β 1 level was 16 to 2,178 ng/mL; the intra- and inter-assay precisions were 2.67 to 6.79% and 4.17 to 6.16% of the CV values, respectively. The range of the assay for serum sFas level was 5.0 to 50 pg/ml; the intra- and inter-assay precisions were 2.18 to 5.55% and 8.24 to 12.30%, respectively. The range of the assay for serum SOD activity was 0.1 to 10.0 U/ml; the intra- and inter-assay precisions were 4.02 to 6.79% and 2.79 to 5.82%, respectively. Mean day-to-day variations (inter-assay precision) of reference sera estimated at the time of measurements for the JACC Study samples were 2.30% for IGF-I, 8.74% for IGFBP-3, 7.51% for TGF-β 1, 7.91% for sFas, , and 8.77% for SOD activity.

Table 2 shows the comparison of serum component levels between fresh samples and samples stored for 6 years at -80℃. There were no apparent differences in serum levels of proteins or

Table 1. Determination method and its precision when serum levels of IGFs, IGF-BP3, TGF- β 1, sFas, and SOD activity in serum samples were estimated by the method used in this study.

Item		IGF-I	IGF-II	IGFBP-3	TGF- β 1	sFas	SOD activity
Assay method		Immuno-radiometric assay (IRMA)	Immuno-radiometric assay (IRMA)	Immuno-radiometric assay (IRMA)	Quantitative sandwich enzyme immunoassay	Enzyme-linked immuno-adsorbent assay (ELISA)	Improved nitrite method (Colorimetric method)
Assay reagents	Company supplied the reagent kit	Daiichi Radioisotope Lab.	Daiichi Radioisotope Lab.	Daiichi Radioisotope Lab.	R&D Systems Inc.	BML Company Ltd.	SRL Lab.
Detection	Ranges (unit)	4-2,000 (ng/mL)	10-1,640 (ng/mL)	0.06-10.10 (μ g/mL)	16-2,178 (ng/mL)	1.0 - 10.0 (pg/mL)	0.1 - 10.0 (U/mL)
Precision	Intra-assay(%)	2.15 - 3.53	2.74 - 4.45	3.16 - 4.19	2.67 - 6.79	2.18 - 5.55	4.02 - 6.79
	Inter-assay(%)	1.12 - 4.18	4.23 - 5.53	5.28 - 8.89	4.17 - 6.16	8.24 - 12.30	2.79 - 5.82
Assay precision	Inter-precision for JACC Study	2.30	-	8.74	7.51	7.90	8.77

Reference serum (CV%): Coefficients of variation were caliculated from the mean values of reference sera estimated by each assay for JACC Study samples.

Table 2. Comparison of serum costituent values in pooled serum determined between 1988 and 1994.

	Year of determination	
Serum component	1988	1994
Total protein (g/dL)	7.5	7.1
Albumin (g/dL)	3.8	4.0
Total bilirubin (mg/dL)	0.7	0.5
Urea (mg/dL)	22	21
Uric acid (mg/dL)	4.9	5.7
Creatinine (mg/dL)	1.5	1.3
Total cholesterol (mg/dL)	209	189
Triglyceride (mg/dL)	121	109
Sodium (mEq/L)	146	146
Potassium (mEq/L)	4.4	4.4
Chloride (mEq/L)	108	102
Inorganic phosphate (mg/dL)	3.9	3.9
Calcium (mg/dL)	8.5	8.0
GOT (IU/L)	16	19
GPT (IU/L)	14	14
LDH (IU/L)	64	75
ALP (IU/L)	52	39
CHE (IU/L)	4,074	3,520
γ -GTP (IU/L)	46	42
LAP (IU/L)	94	77
Amylase (IU/L)	28	23
Autoanalyzer	SMAC (Technicon Co., Ltd.)	TBA (Toshiba K.K.)

1988: data estimated from fresh pooled serum at the time of preparation.
1994: data estimated from pooled serum stored during a 6-year storage at -80℃.

Table 3. Comparison of serum levels of certain cytokines and SOD activity between fresh and frozen samples.

Sample	IGF-I (ng/mL)	IGF-II (ng/mL)	IGFBP-3 (μ g/mL)	TGF- β 1 (ng/mL)	sFas (ng/mL)
Fresh sample	199.8 (21.5)	665.7 (50.9)	3.01 (0.11)	32.99 (3.36)	1.92 (0.23)
N	10	10	10	10	10
Frozen sample	186.2 (12.7)	616.3 (29.7)	3.12 (0.25)	30.44 (2.43)	1.77 (0.22)
N	21	21	21	20	19
Probability	p =0.64	p =0.48	p =0.64	p =0.55	p =0.81

Fresh sample: determination at the time of serum collection in 1999 .
Frozen sample: determination of serum samples collected in 1990 after 9-year storage at -80℃.

Table 4. Comparison of serum levels of IGFs, IGFBP-3, TGF- β 1, sFas, and SOD activity in 100 inhabitants (46 males and 64 females, aged 39-78) collected between 1991 and 1999.

Component		Collected year		Mean
		1991	1999	differences
IGF-I	Mean	167	162	-5
(ng/mL)	25%	130	120	(-3.0%)
	50%	160	150	
	75%	200	200	
IGF-II	Mean	649	652	3
(ng/mL)	25%	570	560	(-0.5%)
	50%	630	660	
	75%	728	750	
IGFBP-3	Mean	3.09	3.03	-0.06
(μ g/mL)	25%	2.72	2.55	(-1.9%)
	50%	3.09	3.07	
	75%	3.52	3.51	
IGF- β 1	Mean	32.3	36.9	4.6
(ng/mL)	25%	22.5	31.6	(14.2%)
	50%	32.0	36.7	
	75%	43.6	42.2	
sFas	Mean	2.44	2.64	0.20
(ng/mL)	25%	1.40	1.6	(8.2%)
	50%	1.70	1.85	
	75%	2.00	2.2	
SOD Activity	Mean	2.9	2.5	-0.4
(U/mL)	25%	1.63	1.8	(-13.8%)
	50%	1.9	2.1	
	75%	2.2	2.5	

Data represented as mean (mean value) and ranges (25%, 50% and 75%).
Mean difference: difference value = 1999-level - 1991-level.
Difference precentages (%) = difference value/ 1991-level.